RF Glass Technology Is Going Mainstream: Review and Future Applications

TOBIAS CHALOUN [1] **(Member, IEEE), SUSANNE BRANDL** [1] **(Graduate Student Member, IEEE),**
NORBERT AMBROSIUS [2] **, KEVIN KRÖHNERT** [3] **, HOLGER MAUNE** [4] **(Senior Member, IEEE),**
AND CHRISTIAN WALDSCHMIDT [1] **(Fellow, IEEE)**

(Invited Paper)

[1] Institute of Microwave Engineering, Ulm University, 89081 Ulm, Germany
[2] LPKF Laser and Electronics AG, 30827 Garbsen, Germany
[3] Fraunhofer IZM, 13355 Berlin, Germany
[4] Chair of High Frequency and Communication Engineering, Otto-von-Guericke-Universität Magdeburg, 39106 Magdeburg, Germany

CORRESPONDING AUTHOR: TOBIAS CHALOUN (e-mail: chaloun@ieee.org).

ABSTRACT Driven by the increasing demand for high-throughput communication links and high-resolution radar sensors, the development of future wireless systems pushes at ever greater operating frequencies. By analogy, high-performance computing (HPC) systems with high-bandwidth I/Os have become a mainstream solution to address multi Gbit/s data rates. Heterogeneous integration technologies play a vital role here in enhancing the performance and functional density, along with reducing the size and costs of such RF systems. In line with this trend, many passive components, which have once been monolithically integrated, are now implemented on ceramic or polymer-based packages. Besides these long-established material and process technologies, considerable efforts have also recently been devoted to the development of RF components on glass and glass-ceramics. Spurred by their low dielectric losses, extremely smooth surfaces, and excellent dimensional stability, glass technologies are emerging as a promising alternative for high-volume and high-performance RF applications. In this article, relevant glass materials and key enabling technologies are reviewed and put into context with well-established RF substrate technologies. Another focus is set on the latest glass-based packaging and interposer solutions ranging from MHz-to-THz frequencies. To showcase the development activities and practical accomplishments of the RF glass technology, also a large variety of key components is presented. Finally, the paper concludes by discussing future research and development directions of RF glass devices.

INDEX TERMS MTT 70th Anniversary Special Issue, glass technology, dielectrics, packaging, interposer, system-on-package, interconnects, filters, antennas, antenna-in-package, millimeter wave (mm-wave).

I. INTRODUCTION

Next-generation wireless communications and sensor technologies increasingly deploy higher operating frequency to enable ultra-miniaturized and feature-rich systems [1], [2]. Similar trends can also be observed in electronic systems such as for high-performance computing (HPC) pushing towards multi Gbit/s data rates [3]. These developments have been spurred by the dramatic advances in semiconductor technologies which meanwhile can absorb a large portion of the system complexity into the integrated circuit (IC) design [4]. Apart from this evolution of monolithic integration techniques,

significant efforts have also been devoted to establishing different substrate material platforms for advanced packaging and component implementations [5].

Rather than following classical IC-centric system concepts referred as system-on-chip (SoC) and system-in-package (SiP), there is an inevitable trend towards heterogeneously integrated system architectures seamlessly combining the strengths of various technologies. Many passive components, which have once been monolithically integrated, are now increasingly incorporated into modern multi-chip-module (MCM) or system-on-package (SoP) designs [6], [7], [8], [9].

Striving for superior system performance and integration density, the off-chip partitioning of lumped/passive components also leads to smaller chip size, lower implementation costs, and enhanced reliability. The proper choice of the material composition is one of the major design challenges here. For packaged as well as discrete RF components, these challenges can be translated into desired substrate characteristics such as low permittivity, low dielectric loss, and low coefficient of thermal expansion (CTE) along with the support of multilayer fabrication techniques with fine-pitch features and high-density I/Os.

Typical material and process technologies to realize passive RF components and interconnects that operate from MHz-to-THz frequencies include low-temperature cofired ceramics (LTCC) [10], organic core/ build-up substrates [11], [12], and high-resistivity silicon [13]. Ceramic-based material systems such as LTCC have long been preferred to realize advanced RF modules and components owing to their support of high layer counts. Moreover, a large variety of different substrate materials with low dielectric losses, high thermal conductivity, and a CTE closely tailored to Si/GaAs semiconductors are available. Therefore, the LTCC technology continues to play an important role even today in high-temperature and high-reliability RF applications [14]. From the present perspective, however, multilayered ceramics are limited in terms of their integration density and performance due to material shrinkage during cofiring, low feature-size on internal metal layers and the poor electrical conductivity of the cofired metals [5], [15]. These limitations and the prohibitive fabrication costs of ceramic substates have recently led to the prevalence of multilayered organic substrates in commercial RF applications.

In conventional PCB processes, a composition of copper-cladded laminates and prepregs are bonded together to form low-cost multilayered organic substrates. The mainstream RF materials can be categorized into four classes of polymers: PTFE (polytetrafluoroethylene), PPE (polyphenylene), bis-maleimide triazine (BT), and liquid crystal polymers (LCP). Unlike their ceramic counterparts, they are compatible with high-volume commercial manufacturing and packaging techniques due to their large-panel scalability. On the other hand, conventional PCB technologies still pose the design challenge in providing small feature sizes induced by the limitations of the subtractive wet etching process and the layer-to-layer registration tolerances. In addition, the relatively thick laminates prevent the down scaling of microvias. These constraints eventually led to the proliferation of organic build-up substrate process technologies enabling complex signal routing and high-density interconnects essentially for HPC and millimeter wave (mm-wave) applications [16], [17].

Despite these advances, however, silicon-based interposers and packages are still unmatched in terms of their wiring and I/O density as a result of the thermomechanical process limitations of organic substrates from their low modulus and high CTE [5]. Silicon substrates with sub-micron back end of line (BEOL) redistribution layers (RDLs) and through-silicon vias (TSVs) are currently the most advanced and most commonly used interposers [18]. Silicon interposer technologies are primarily used in high-performance computing applications interconnecting logic blocks and high bandwidth memories (HBMs) in an ultra-dense fashion. The CTE of silicon interposer substrates and silicon-based ICs only insignificantly deviate from one another, which effectively mitigates warpage in vertically stacked ICs. Although this technology enables excellent power bandwidth scaling at system level [19], silicon interposers are attributed with high manufacturing costs due to the limited wafer size. In addition, they face significant signal-integrity issues at higher operating frequencies above the single-digit GHz range as a result of the finite conductivity and the relatively high permittivity of this semiconductor material.

Another disadvantage can be found in nonlinearity of conventional TSVs through the formation of a metal–oxide–semiconductor capacitor. Hence, silicon substrates are very unfavorable for high-linearity and low-insertion loss RF applications [20].

In recent years, glass and glass-ceramics have emerged as a superior alternative to these well-established substrate materials for electronic devices [21], [22], [23]. While the development of glasses has been optimized for the use in optical instruments over centuries, glass materials had no significance – apart from military-grade feedthroughs and connectors [24] – for a long time in RF applications. The reason for this was the immaturity of process technologies to reliably realize fine conductor tracks and vias, along with the lack of suitable chip integration techniques. A radically different situation from 15 years ago, nowadays various through glass via technologies have been investigated including mechanical, laser, and gas-discharge drilling as well as hybrid technologies combing wet etching and laser drilling [15] (see Section II-B). Furthermore, silicon-like RDL wiring on glass panels has become feasible by extending semi-additive process (SAP) methods once developed for fabrication of BEOL layers on chips [25]. In retrospect, these technological pillars have been spurred by the unique properties of glass materials which combine the advantages of organic and silicon substrates. The excellent dimensional stability and smooth surface roughness of glass enable fine-pitch lines/spaces as well as high aspect ratio TGV formations. Glass substrates also owe their popularity because of their ability to provide low-loss dielectric properties far beyond the mm-wave regime [21]. Another reason can be found in the high coplanarity, tailorable CTE, robustness to high temperatures, and high reliability of glass substrates which facilitate the use of panel-level manufacturing and packaging processes at low costs. Although there is still a lack of material and assembly supply chain readiness [26], the current level of process maturity has led to numerous demonstrations of components, packages, and interposers using glass substrates from both industry and academia [27], [28], [29], [30].

This contribution reviews the current glass related developments with particular emphasis on RF applications. The paper is organized as follows: Section II gives a brief overview on state-of-the art glass technologies, while Section III

discusses the latest developments on glass-based packaging and interposer solutions. Subsequently, the paper reviews various RF component designs, which deploy glass materials, in Section IV. Rather than surveying the entire glass component landscape, we focus on four building block categories commonly applied in RF systems: I) transitions and interconnects, II) filter and resonator, III) phase shifters, IV) antennas and periodic structures. Finally, Section V discusses some future prospects of glass technologies in the realm of RF applications, followed by a conclusion and outlook.

II. GLASS TECHNOLOGIES

A. MATERIAL OVERVIEW AND CHARACTERIZATION

Fused silica is a synthesized glass material of almost pure silicon dioxide (SiO_2). It can virtually be made free of impurities along with an extremely high degree of homogeneity. Hence, this amorphous dielectric naturally provides excellent transmission properties up to frequencies in the UV range. Specifically regarding the mm-wave spectrum, different fused silica substrates have recently been characterized in [31] up to 110 GHz by means of a loaded disc resonator showing very constant permittivity and loss tangent values of ϵ_r=3.8±0.1 and $tan\delta$=1.5–5 × 10^{-4}, respectively. Among other inorganic substrates for sub-THz and THz components, similar electric properties for fused silica have been reported in [32] across the frequency range from 0.5 THz to 6.5 THz using THz time-domain spectroscopy. Moreover, fused silica – like many other glass materials – features of high chemical and thermal resistance [33], [21], but the downside is its relatively low CTE for using in heterogeneous integration technologies.

By incorporating chemical elements into the amorphous glass composition, the CTE can be adjusted over a wide range to match other packaging materials [34]. However, the change in the glass composition also has an inevitable impact on electrical properties. For instance, the addition of alkali ions is an effective method to increase the thermal expansion coefficient of silicate glasses, but at the expense of higher dielectric losses due to increased ionic conductivity [35]. Note that alkali-reduced borosilicate glasses can achieve a loss tangent as low as 2 × 10^{-2} at microwave frequencies [36], [37], while alkali-free borosilicate substrates can even be engineered with a loss tangent less than 1 × 10^{-2} in the mm-wave regime [38].

Glass ceramics may further extend the parameter range of glass compositions, while maintaining the excellent homogeneity of glass. They are made by annealing precursor glass which subsequently undergoes a specific heat treatment schedule to control the nucleation and crystallization process. Since the crystallization process typically does not fully complete, glass ceramics contain both a crystalline and a small residual glass phase [39]. As a consequence, the dielectric properties of glass ceramics can be controlled by its glass composition as well as its crystalline structure and phase assemblage. These additional degrees of freedoms allow, for instance, the realization of ferroelectric glass-ceramics with very high permittivity values of ϵ_r=32 and beyond [34]. In

TABLE 1. Comparison of Different Glass and Glass-Ceramic Materials for RF Applications Including Some Standard PCB/LTCC Substrate as a Reference Point

Material	ϵ_r	$tan\delta$ (10^{-4})	CTE (ppm/K)	Ref.
Fused Silica	3.8 @ 20 GHz	2 @20 GHz	0.5	[31, 33, 41]
Schott Borofloat33	4.5 @20 GHz 4.5 @20 GHz	120 @ 24 GHz 130 @ 77 GHz	3.25	[42, 34]
Schott AF32 eco	5.0 @ 24 GHz 5.1 @ 77 GHz	90 @ 24 GHz 110 @ 77 GHz	3.2	[38]
Schott D263T	6.3 @ 24 GHz 6.1 @ 77 GHz	210 @ 24 GHz 240 @ 77 GHz	7.2	[36]
Schott MEMpax	4.4 @ 24 GHz 4.4 @ 77 GHz	100 @ 24 GHz 150 @ 77 GHz	3.3	[37]
Corning 7059	5.75 @ 10 GHz	36 @ 10 GHz	4.6	[43, 33]
Corning 7070	3.9 @ 25 GHz	31 @ 25 GHz	3.2	[33]
Corning 7740	4.52 @ 25 GHz	73 @ 25 GHz	3.25	[33]
Corning 7900	3.82 @10 GHz	9.4 @ 10 GHz	8	[43, 33]
Skyworks D-4 Cordierite	4.5 @ 9.4 GHz	2 @ 9.4 GHz	2	[44]
Rogers RO3003	3 @ 10 GHz	10 @ 10 GHz	17 (xy) 25 (z)	[45]
Panasonic Megtron7	3.31 @ 14 GHz	23 @ 14 GHz	15 (xy) 42 (z)	[46]
Ferro A6M-E	5.7 @ 10 GHz	10 @ 10 GHz	7	[47]

the realm of RF applications, their practical use is, however, limited to frequencies in the lower GHz range due to severe dielectric losses above this spectral region. Compared with this, cordierite has emerged as a promising dielectric for microwave and mm-wave components with relative permittivity between 4.9 to 5.5. Among all reported glass-ceramics, cordierite shows the lowest loss tangent of around 2 × 10^{-4} at mm-wave frequencies [40], [21]. It is interesting to note that the dielectric losses of cordierite glass-ceramics are of the same order of magnitude as that of fused silica. A comparison of different glasses, glass-ceramics as well as some standard PCB/LTCC laminates for RF applications is given in Table 1.

B. GLASS PROCESSING TECHNOLOGIES

To enable glass micromachining, various technologies are available and have been evaluated. The most state-of-the-art production processes are CNC based mechanical abrasion processes like drilling, milling, powder-blasting and grinding which are used in high-volume manufacturing e.g., for display cover glasses. Nevertheless, these processes are limited in feature size and available aspect ratio. Furthermore, these mechanical processing generate defects like chipping and microcracks that significantly reduce the mechanical stability of the substate. Laser based processed like direct ablation with ultra-short-pulsed (USP), pulsed UV, CO_2 or Excimer Lasers have been used to process glasses, by applying a multitude of focused laser pulses to ablate the material. In case of USP, UV,
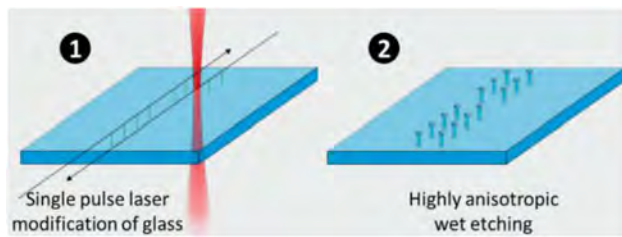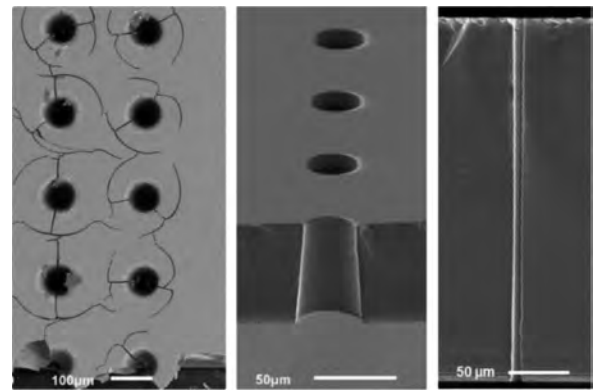
FIGURE 1. LIDE two-step process: 1) single pulse laser modification of the whole glass thickness, followed by 2) unmasked batch wet-etching with highly anisotropic wet etching of the laser-patterned regions to form the TGV [176].


FIGURE 2. Examples of through holes with direct laser ablation (left) and LIDE processing (center and right picture). The sample on the left was dipped in hydrofluoric acid to reveal microcrack induced by thermal stress.

and CO_2 lasers the focused laser beam is usually moved with a galvanometer scanner that enables highly flexible processing with good accuracy, but throughput is limited because each feature is sequentially processed and the processed features have a heat-affected zone with high thermal stress that can lead to microcracks. Excimer Laser ablation is a mask-based process and therefore can potentially achieve high throughput values but each layout needs an individual mask. Beneath laser and mechanical processes masked wet etching is commonly for glass processing, especially in MEMS production to generate cavities e.g., for sensor packaging. Since the applied wet etching process is isotropic only low aspect ratios smaller than 1:1 can be achieved. A detailed description and summary of the above-mentioned glass processing technologies can be found in [7].

In many cases high-frequency applications need precisely manufactured substrates with high aspect ratios which at reasonable production cost. To overcome the limitations of the described processes, hybrid processes that combine a laser process with wet etching processes have been developed. One of these processes is Laser Induced Deep Etching (LIDE) [48], [49]. This process uses a laser modification that can be defined by one single laser pulse through the full glass thickness, which etches highly anisotropic in a subsequent wet etch process (see Fig. 1).

LIDE is a direct write laser process which makes it highly flexible and can precisely define several thousand modifications per second. Multiple features like through holes, blind holes, cavities, and larger cutouts can be generated in one process step [50]. These features are defect free which results in a high mechanical stability of the substrate [51]. Fig. 2 shows exemplary holes drilled through glass with an ultra-short-pulsed laser that have subsequently been dipped in hydrofluoric acid. The short etching step reveals the microcracks that have been induced by thermal stress during processing. In comparison, the through-glass vias shown in the center and right picture, respectively, have been processed with the LIDE process.

Micro-electronic packages are often composed of several substrate layers which must be bonded to each other. Several bonding processes are available, that depending on the substrate and bond specifications have individual benefits and drawbacks [52], [53], [54]. The most common processes

for semiconductor related applications are Polymer, anodic, direct/fusion, metal (e.g., solder or eutectic) and glass-frit bonding. In some cases, an adhesion bond where a polymer layer is spun on one of the substrates and then connected to the second substrate is sufficient but is very limited in maximum temperature. Anodic bonding can be used to bond silicon to glass or, typically with a thin intermediate layer, glass to glass and enables a highly stable and hermetic sealing of the bonding partners but is limited to alkaline glasses [55].

Direct bonding can be used with all available types of glass but requires a very low surface roughness (Ra < 1 nm). The substrates are pre-bonded at room temperature, followed by an annealing process to increase the bond strength [56]. Metal bonding processes are more tolerant to surface roughness. Eutectic bonding is defined by two metals, one on each bind partner, that alloy to an intermediate phase at rather low temperatures, for example Indium and Gold that have a eutectic temperature of 156 °C [57]. Beneath the bond of the substrates a conductive connection of redistribution layers can be done in parallel. Like polymer bonding, glass-frit bonding, which uses a low melting point glass paste as an additive, can compensate for high surface roughness. The most recent bonding process is laser direct bonding which uses a tightly focused ultra-short-pulsed laser beam that is applied at the interface of the bonding partners which locally liquifies the material [58], which enable hermetic packaging of temperature sensitive components.

C. METALLIZATION

The metallization of TGVs is typically based on the same approach and is using the same machines which are in use for TSV interposer fabrication. Hence the TGVs are typically metallized by using physical vapor deposition (PVD), chemical vapor deposition (CVD) or electroless deposition for a seed layer inside the via [59], [60]. Other approaches would be using Schott Hermes Glass with integrated tungsten plugs or using pastes, solder or powder to create a conductive path through the wafer [61], [62], [63].
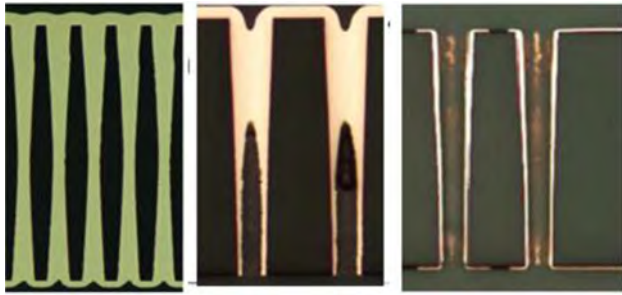
FIGURE 3. From left to right: Fully filled TGVs (50 μm diameter, 470 μm thickness, plugged TGV (70 μm diameter, 460 μm thickness), liner plated TGV (70 μm diameter, 460 μm thickness).

Depending on the via dimensions and the thickness of the interposer, different metallizations are possible. For RF applications, a high conductive copper metallization with a low roughness is favorable [64]. Depending on the geometry of the interposer (thickness, via diameter, via pitch) different metallization concepts which could form a conductive path through the wafer are possible. This could be divided into fully filled vias, liner plated vias or plugged vias which are not fully filled. However, since they form a plug inside the vias, a hermetical sealing is still guaranteed [65]. In Fig. 3, selected samples of those variants are shown. In an exemplary way the creation of an interposer with several redistribution layers is discussed in the following. Depending on wafer thickness and via dimensions the fabrication of such interposer when using PVD/CVD or electroless deposition can be seen in Fig. 4.

A glass interposer fabrication process glass starts with the realization of slightly tapered holes (1.5°) using the LIDE process (Step 1). Depending on the target via diameter, wafer thickness, pitch and application different technological approaches A and B are possible. While approach A is well suitable to handle thin glass wafers (< 300 μm), approach B allows to process thicker glass wafers with higher aspect ratios (via diameter/ wafer thickness) but is more complex to fabricate (double-sided via filling). In both cases, the vias are filled in the first step and overburden (excess copper on the wafer) is removed, creating a glass wafer which has only the desired metallization inside the via [66], [67], [68] (Step 2). In the following step the top or bottom side can be fabricated. Typically, the side which has the lowest topography after processing (only pads) is processed first. This is typically a combination of different routing metallizations with a passivation in between. Typically, pads which are compatible for soldering the interposer to a PCB are formed for the final layer [69], [67] (Step 3). Subsequently, the other side – typically the frontside of the wafer – is processed. For approach A the interposer is now bonded to a carrier wafer to support the still stable glass wafer (Step 4). The glass wafer is now thinned down to its desired thickness and the backside TGV openings are exposed making it possible to create the necessary structures on the frontside (Step 6). After the finalization, the carrier wafer gets de-bonded and the interposer cleaned (Step 7). For approach B, the frontside can be directly fabricated
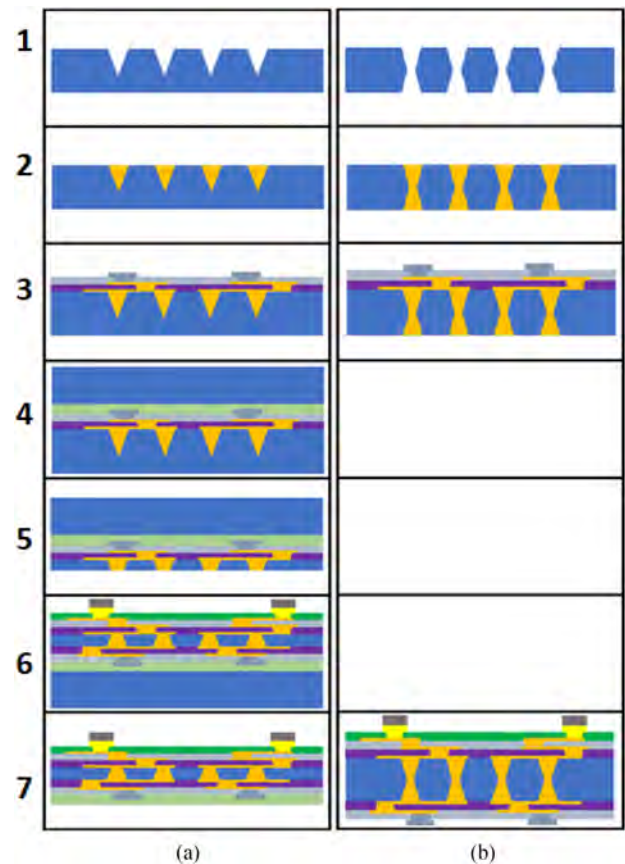
FIGURE 4. Example of possible processing flows depending on glass wafer thickness and capabilities of the facilities.

with different routing and passivation layers without using a carrier wafer due to its stability [18].

III. PACKAGING AND INTERPOSER SOLUTIONS

Heterogeneous integration technologies play a decisive role in developing feature-rich, ultra-compact microwave and mm-wave systems. Since transistor downsizing is going to reach its economical and physical limits, there is a clear paradigm shift towards advanced 2.5D and 3D packaging solutions to scale the performance of complex microsystems [15]. In light of this trend, various materials and process technologies have been established to provide ultra-dense multi-chip packaging and wiring [70]. This includes, but not limited to, low-temperature cofired ceramics (LTCC) [10], [71], organic (core/ build-up) laminates [72], [11], [17], silicon [3], [73], and embedded wafer fan-out packages with epoxy molding compounds [74], [75].

In recent years, glass-based packages and interposers have evolved as a serious alternative to these technologies mainly because of their ability to provide low-loss electrical properties in the mm-wave and Sub-THz regime, fine-pitch lines and spaces as well as high aspect ratio TGVs.

In the last decade, considerable efforts have been devoted to glass-polymer packages aiming to leverage the advantages of both material systems [76], [26]. This hybrid packaging
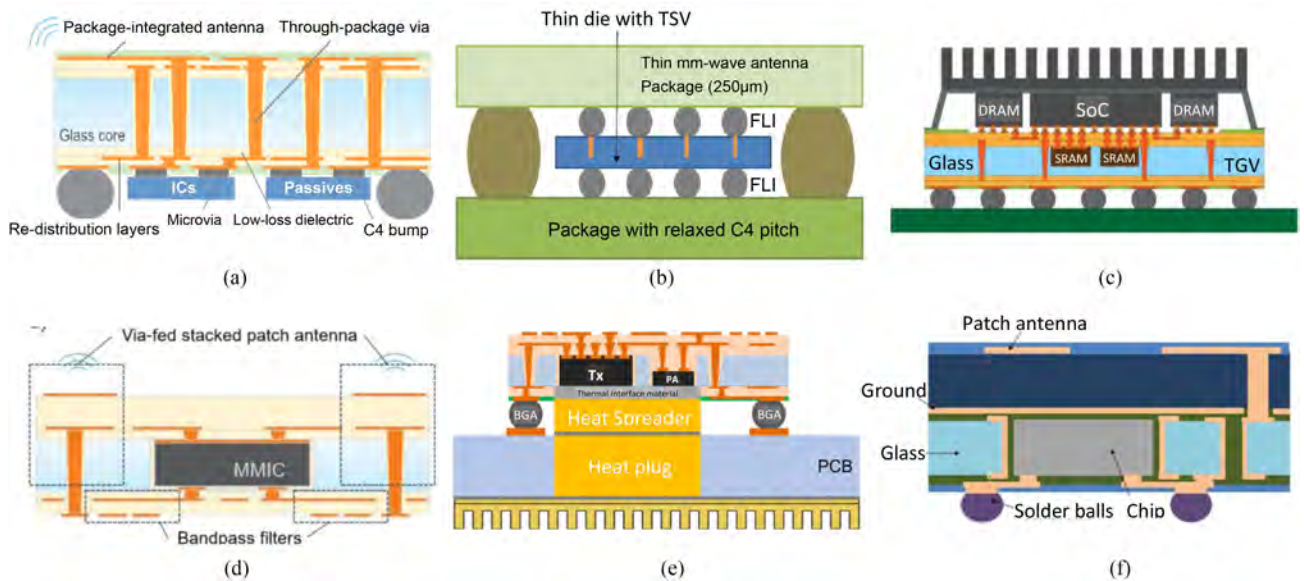
FIGURE 5. Glass-based packages and interposers a) 2.5D glass-polymer package for mm-wave applications (28 GHz) [26] b) Bare glass interposer [29] c) 3D GPE package for HPC [80] d) 2.5D GPE package for mm-wave 5G (28 GHz) [85] e) 2.5D GPE package for 6G applications (170 GHz) [88] f) 2.5 GPE mold compound package for mm-wave radars (77 GHz) [84].

approach utilities an ultra-thin glass core onto which organic build-up films are laminated and metal layers are patterned by means of a conventional SAP process (see Fig. 5(a)). In this way, the active and passive components accommodated in the package can be densely interconnected with transmission lines, microvias and TGVs. From the mechanical point of view, the thin-film laminates have an equally important function in absorbing the brittleness of thin glass substrates. On the other hand, bare glass interposers without polymer-based RDLs feature lower dielectric losses, less fabrication steps, and compatibility with very cost-effective high-volume TGV formation techniques [20], [77], [78]. As an example, Fig. 5(b)) shows the cross-sectional view of a mm-wave package which uses a 2-layer photodefinable glass substrate to implement the antennas and feeding lines at 60 GHz [29].

Besides chip-last architectures, in which the ICs are finally assembled on top or bottom of the package, various concepts of chip-embedded glass packages have been studied as a potential solution for much higher I/O counts and more versatile application-specific integration capabilities. The first 2.5D glass panel embedded (GPE) package for interconnecting logics and high bandwidth memories in high-performance computing has been reported in [79]. In conjunction with the organic RDLs, whose formation is conducted after the die-embedding process, the chip interconnects can achieve BEOL-like I/O densities on package level. From the technological perspective, the reason can be found in the excellent dimensional stability of glass and the ultra-short microvias which are directly plated onto the IC pads. By contrast, current silicon interposers and mold compound embedded packages are not able to compete in terms of I/O pitch, bandwidth, and reliably owing to thermo-compression bonding assembly and

die shift induced limits [19]. More recently, several 3D glass-based package architectures for HPC applications have been demonstrated in [80], [81], [82]. The advanced 3D package concept as illustrated in Fig. 5(c) expands the GPE technology to support chip-embedded and flip-chip integration techniques. Since the embedded ICs are integrated face-up into the glass panel along with the flip-chip ICs on top of the RDL, ultra-short and ultra-dense interconnects across chiplets can be realized without reverting to use inefficient TSVs [20]. The very favorable mechanical and electrical characteristics of the polymer-enhanced GPE technology has also led to multifaceted developments of mm-wave antenna-integrated packages [83], [84], [26]. A 28-GHz antenna-integrated package for 5G communications was demonstrated in [85]. The layer stack-up (see Fig. 5(d)) consists of multiple RDLs on top and bottom of a glass embedded panel using an organic build-up substrate technology. The radiating elements and their feeding structures are integrated on the top side of the package, while the filters and the fan-out of the baseband signals are realized on the bottom side in order to prevent the degradation of the radiation characteristics. Following a similar package configuration, a multi-die automotive radar module at E-band has been proposed [86].

Current research indicates that this die-embedded glass package technology may also be suitable for future 6G wireless communications at D-band [87], [88]. An example of a sub-THz glass-polymer package with integrated antennas and microvia chip-to-package interconnects is shown in Fig. 5(e). By leveraging the benefits of the microvia technology supporting via diameters below 5 μm with pitches of 8-12 μm [89], low insert losses for these cross-technology interconnects could be demonstrated at D-band. Moreover, the proposed
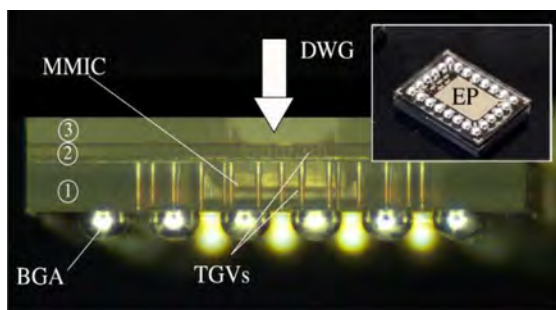
FIGURE 6. Side view of a hermetically sealed glass embedded package for sub-THz radar applications [93].

packaging and assembly concepts ensure efficient heat removal along the vertical direction to address the excessive heat dissipation from D-band power amplifiers. Both aspects become increasingly important in designing scaled phased array antennas at submillimeter-wave frequencies through functional partitioning [90], [2].

Hybrid packaging solutions with glass substrates and molding compounds also find applications in the mm-wave range to enhance the reliability of wafer-level fan-out technologies [91], [92]. Fig. 5(f) provides an example of a glass-embedded package composed of a conventional RDL to form the fan-out area and a molding compound on top of the glass core for the antenna elements [84]. The ability to process thicker dielectrics for the radiating elements at 77 GHz helps to meet bandwidth and efficiency requirements. A radically different approach has been pursued by the authors of [93] presenting the first multilayered chip-embedded glass package for radar applications at 150 GHz (see Fig. 6). Since this package is solely based on glass substrates, plated TGVs, and a circulating solder ring, a hermetically sealed encapsulation of the RFIC is ensured, which play a vital role in application scenarios with harsh environmental conditions. Another distinguishing feature is the ultra-compact transitions from the RFIC to a dielectric waveguide (DWG) whose superior RF performance stem from use of high-aspect ratio TGV in conjunction with a state-of-art microbump technology.

IV. COMPONENTS

A. TRANSMSSION LINES AND INTERCONNECTS

The properties of transmission lines and interconnects have crucial influence on the performance of electronic systems. While conventional RF systems set priorities on precise impedance control and low insert loss in this regard, HPC systems, on the contrary, emphasis more on high I/O counts and large transmission bandwidths. However, emerging HPC systems with multi Gbit/s data rates or massive MIMO RF communications systems increasingly require to deal with both small feature size and impedance control. In particular for higher operating frequencies, this becomes a major and ubiquitous design challenge for conventional materials systems (see Introduction), whereas glass-based substrate

technologies are envisioned to close this gap through its excellent electrical, thermal and mechanical properties (see Section II).

A large variety of planar transmission line techniques on glass and glass-polymer substrates have been reported such as microstrip lines [94], coplanar waveguides (CPWs) [95], [96], [97], and their derivates [98], [94] showing excellent RF characteristics beyond 150 GHz.

Vertical RF signal routing through the glass substrate using TGVs are often formed as three-wire lines [28], [20], [26] and quasi-coaxial lines [50], [93]. Moreover, even multilayer glass configurations with stacked TGVs are possible, whose galvanic contacts can be established by Cu/Sn bonding (see Fig. 7(a)) [99] or conductive paste [100].

In contrast to their planar counterparts, the technological hurdle for realizing substrate integrated waveguides (SIW) in glass is higher as they include many densely packed TGVs, which in turn places stringent requirements on the via process. Despite this, glass materials are getting more popular to implement SIW transmission lines, in particular at mm-wave and sub-THz frequencies, not at least due to the low dielectric losses and high metallization quality of this technology [50], [101], [102]. Fig. 7(b) exemplary shows SIW transmission lines in a polymer-glass-polymer configuration exhibiting insertion loss between 0.5 dB/mm to 1 dB/mm across the entire D-band. Moreover, dielectric waveguides (DWGs) have recently gained renewed attenuation to alleviate high signal attenuation at mm-wave frequencies, since ohmic losses are avoided. While most of the reported DWGs for mm-wave applications are made from low-loss organic materials [103], [93], [104], first developments of DWGs in borosilicate glass were presented in [105] for the use in high-temperature and chemical-hazard environments.

More recently, a new silicon-on-glass (SOG) technology has been presented for low-loss and low-cost sub-THz and THz applications [106], [107]. This class of waveguide is typically composed of a high resistivity silicon wafer bonded onto a glass substrate. The formation of transmission lines and components are made via deep reactive ion etching (DRIE) of the silicon bulk. The experimental verification of a SOG-based ridge dielectric waveguide shows attenuation characteristics less than 0.19 dB/cm up to 170 GHz [106]. A suspended SOG waveguide configuration has demonstrated in the frequency range from 500 GHz to 595 GHz in [108], where higher order modes are suppressed by etching the glass substrate below the silicon guiding channel (see Fig. 7(c)).

Package-to-board transitions are conventionally implemented either using wire-bonding [109] or flip-chip techniques [110], [111], [92]. Fig. 7(d) exemplary shows an MSL-to-CPW transition for flip-chip packages up to 40 GHz [28]. In this design, the CPW was realized on glass, whereas the microstrip line was structured on the PCB. The galvanic connections between the organic and glass substrates are provided by solder balls with a diameter of 400 μm. In a similar fashion, copper-pillar techniques have become well established for chip-to-package interconnections reaching I/O
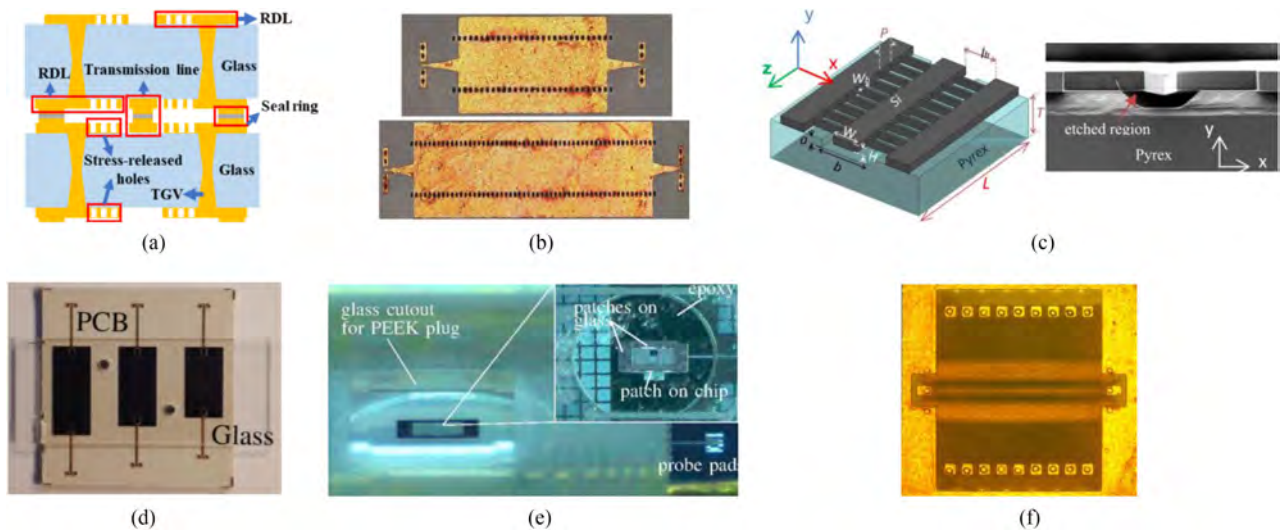
FIGURE 7. Transmission lines and interconnects using glass technologies (a) Vertical RF transition based on TGV stacking and Cu/Sn bonding [99] (b) SIW transmission lines with 4mm/8mm length [101] (c) Suspended silicon-on-glass waveguide [108]. (d) MSL-to-CPW transition up to 40 GHz [28] e) Electromagnetically coupled chip-to-package transition f) Microvia-based chip-to-package transition [88].

pitches of less than 40 μm for bump sizes in the range of 20–25 μm [5].

While advanced micro-pillar interconnects were initially developed for HPC applications to meet high I/O densities, this technology is also widely used nowadays in mm-wave and Sub-THz package designs. In [50], a high-performance transition between the on-chip microstrip line and the SIW section on glass has been demonstrated at D-band using a quasi-coaxial configuration in a 50-μm microbump technology. Following a similar design approach, a vertical microbump transition found application in [93] to realize a broadband galvanic contact between the radar transceiver IC and the slot-loaded patch element in the package, which in turn excites a DWG transmission line. Another popular technique is the use of RF interconnects which relies on electromagnetic field coupling [112], [113]. Since, as a matter of principle, these transitions do not necessarily require TGVs or solder-based bumps, the manufacturing process is typically easier and more cost-effective. On the other hand, galvanically isolated transitions typically suffer from relatively large dimensions – in the order of a quarter wavelength – restricting their use on chip- and package-level at the mm-wave frequencies and beyond. Fig. 7(e) shows an electromagnetically coupled chip-to-package transition at D-band [93]. It consists of a short-circuited quarter-wavelength patch on the chip, whereas the complementary part within the glass package is based on a stacked patch arrangement.

Aiming to provide higher integration densities through GPE packages (cf. Section III) has also led to the development of various vertical interconnects for mm-wave applications up to the D-band. This includes via-in-via through package transitions. This includes chip-to package microvia transitions (see Fig. 7(f)) which land from the thin build-up layers directly onto the chip pads [85], [86], [19], [81], [88]. Via-in-via

through package interconnects [26], [80], [81] and microvia-enhanced organic RDLs on glass core substrates [114], [115], [116] were also reported for future HPC and wireless communications systems.

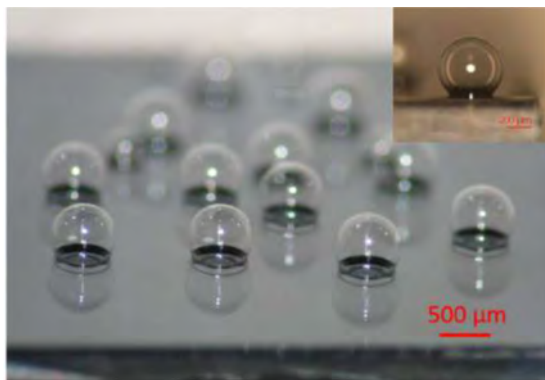## B. RESONATORS, FILTERS, AND PHASE SHIFTERS

Glass is particular favorable for RF components with stringent Q-factor requirements such as filters and resonators. One of the main reasons is that glass features low dielectric loss and more importantly smooth surface roughness (see Section II-A). The latter one allows to realize RF components with significantly reduced conductor losses compared to other materials such as PTFE-based laminates [27]. As a matter of principle, this effect gains significance at higher operating frequencies.

There are mainly two options to implement glass-enhanced RF components and circuits. The most straight-forward one is to use the glass as a replacement for common substrate materials [27], [117]. Here, the technology of SAP, e.g., from LCD panel fabrication can be used to mass produce RF components of (almost) any size at very low cost. For the production of small batches, standard cleanroom techniques such as metallization, lithography, etching and electroplating can be used to realize components with the smallest features and highest precision (see Section II-C). Mm-wave, sub-mm-wave, and even THz-components benefit from the outstanding precision available in glass technologies. Examples are the integration of Schottky diodes into split-block waveguides [118], [119], [120], [121]. Fig. 8 shows the example of a subharmonic mixer at 220 GHz with the co-integration of active Schottky diode and LO/IF filters on a single glass substrate. The quartz glass is mounted into a metallic split-block forming the waveguides for the different signals.
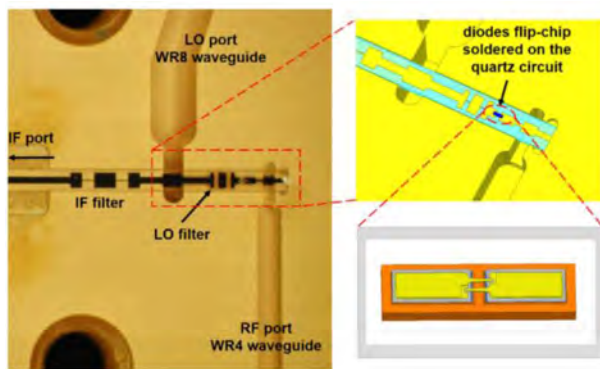
FIGURE 8. Subharmonic mixer at 220 GHz with a Schottky diode mounted onto a glass substrate which is later mounted in a brass split block with the WR8 and WR4 waveguide connections [119].

FIGURE 10. Filter from [131] (left) CAD model view with the three-layer glass-based (yellow) filter and the split-block assembly (gray) for measuring purposes. The waveguide cavities are highlighted in blue. (right) assembly of the filter with top glass removed.
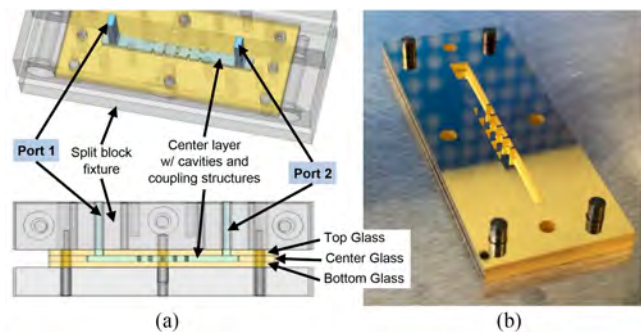

FIGURE 9. Array of whispering gallery mode resonators made from microspherical glass shells. The resonance is at around 400 THz with a quality factor of 10^6 to 107 [125].

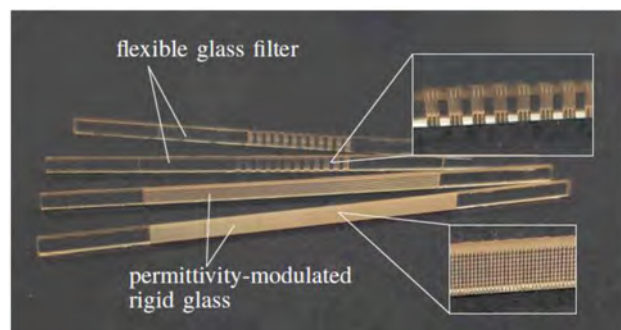**FIGURE 11.** Filter from [105] using holes to locally modulate the effective permittivity.

Recently, glass materials are also used as a dielectric load for resonators. These are realized in different technologies such as substrate integrated waveguide [122] at X-band and substrate integrated coaxial resonators [123] and K/K_a-band, respectively. These structures make direct use of the dielectric properties of the glass substrate. Another approach has been followed in [124] in which the authors integrated inductors with TGVs into the glass substrate and combined them with chip capacitors to synthesize a bandpass filter.

Whispering gallery mode resonators are known for extraordinary quality factors and have been intensively used in optics. In [125], the authors present an array of microspherical glass shells resonating at 400 THz which has been realized with a wafer-scale glass blowing techniques as shown in Fig. 9. More specifically, the bubbles are realized through bonding of a silicon and a borosilicate glass wafer with air cavities at the place of the microbubbles which are inflated afterwards in a vacuum oven at 775 °C. Potential applications are nanoliter liquid sensing, e.g., for bioanalyte detection and lab-on-a-chip applications [125], [126] or high-resolution magnetometers [127].

At lower frequencies glass resonators usually are based on cylindrical bulk bodies. Beside aforementioned applications,

glass is commonly used as resonator confinement in dielectric (resonator) antennas [128], [129], [130].

Machining of bulk glass to realize filter functions is a recent technique. Here, laser-induced bulk micromachining can be used to realized complex structures with the highest precision and feature sizes, in particular holes, as small as 30 μm. The authors of [131] present a glass-integrated W-band filter based on rectangular waveguide cavities (see Fig. 10). The structure is manufactured with laser induced etching (cf. Section II-B) in three separate layers (top with source and load coupling, center with the resonant cavities including their coupling structures, and unstructured bottom). After metallization with Cr/Au by sputtering the wafers are thermo-compression bonded at 250° for 2.5 hours. The advantage of smooth surfaces could be confirmed after metallization with measured surface roughness in the order of 250 nm and 800 nm for the wafer surface and for the side walls of the cavities, respectively.

As ohmic losses become more significant at higher frequency and waveguides' dimensions become critical for manufacturing, the transition to dielectric waveguides is a viable option for sub-mm and THz applications. The authors of [105] used glass for the formation of a dielectric waveguide and modulated its permittivity along the line to realize a filter at G-band (140–220 GHz) as shown in Fig. 11. The glass rods are modified with holes to locally reduce the permittivity
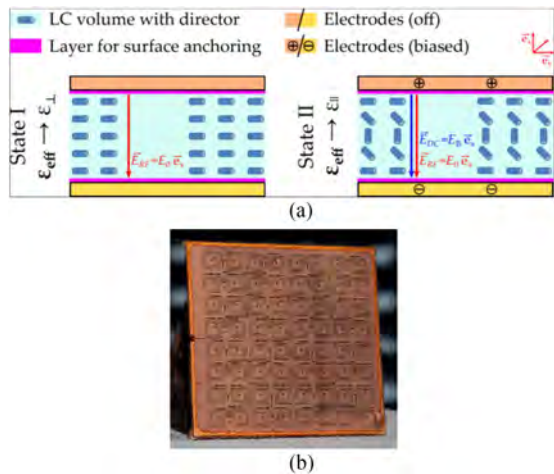
FIGURE 12. (a) Microstrip transmission line utilizing the anisotropy of LC for the realization of a phase shifter. (b) 8 × 8 prototype realized in thin film LC technology [138].

FIGURE 13. (a) Glass substrate with the CRLH transmission line and ground brass block and (b) zoomed view of the periodically repeated CRLH with highly resistive NiCr lines for electric biasing [138].

FIGURE 14. Transparent patch antennas. (a) Meshed copper on flexible Corning Willow at 1 GHz [144], (b) meshed aluminum on quartz substrate at 77 GHz [148], (c) ITO on soda-lime glass at 2 GHz [149].
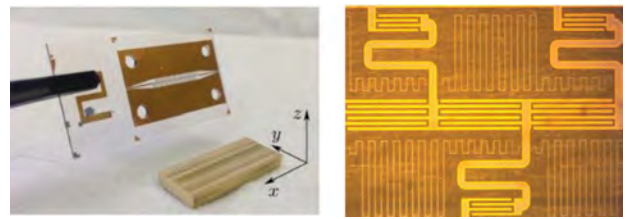
resulting in a waveguide with filtering properties. Additional meandering slots allow for bending of the waveguide. The processing is carried out by laser structuring and a subsequent wet etching step. Especially the latter examples show the potential of the glass technology e.g., for the implementation of advanced functionality into packages/interposers (cf. Section III).

As the realization of low-loss transmission lines in silicon is challenging, glass substrates are also used in conjunction with semiconductors materials on wafer-level to create off-chip circuitries such as filters with low-loss characteristics. In [132], an inverted microstrip line technology for filters has been presented in which the ground plane is realized on a glass wafer, whereas the stripline has been structured on a silicon wafer prior bonding them together.

Owing to their encapsulating features, this technology is also extensively used to hermetically seal sensitive components such as RF-MEMS [133], [134] and for monolithic microfluidic devices [135], [136].

A combination of both microfluidic structures and glass is used in the realization of phase shifters based on liquid crystals (LC) [137]. Here, the LC is used as a tunable dielectric to change the phase constant of a transmission line as illustrated in Fig. 12(a). This concept has been demonstrated in [138] for the realization of a passive electronically steerable antenna. The 8 × 8 antenna array with LC-based phase shifters is depicted in Fig. 12(b). As these antenna systems are physically large, advanced manufacturing methods from LCD-panel fabrication can be adopted accordingly.

A similar assembly is used in [139], [140] for the realization of impedance-controlled surfaces to create tunable leaky wave antennas. The slow wave structure for radiation is realized with a metamaterial based on composite right/left-handed (CRLH) unit cells (cf. Fig. 13). The glass substrate holding the CRLH line is mounted onto a brass carrier to create an air cavity. The cavity is subsequently filled with liquid crystal
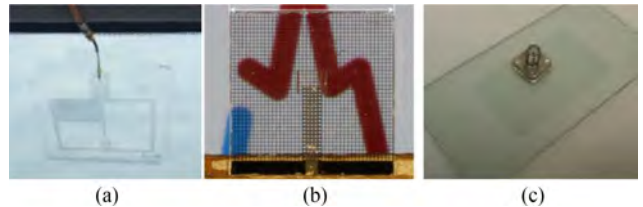
to electrically tune the permittivity of the line. With different phase velocities of the line, the steering angle of the leaky wave antenna can be adjusted.

C. ANTENNAS AND QUASI-OPTICAL STRUCTURES

Optical transparency is a key feature when integrating antennas above solar panels to cope with limited area in space-borne communication systems [141], [142]. Transparent antennas and periodic structures can also be employed for smart glasses [143], vehicle-to-vehicle or vehicle-to-network communication [144], [145], e.g., mounted on the windshield (see Fig. 14(a)), and for improving cellular and WLAN coverage in urban areas [146], [147]. Employing flexible glass, such as Corning Willow substrate, integration with curved windows is possible [144]. To allow for good optical transmittance, transparent metallization is required as well as a transparent substrate material. This can be achieved by either a meshed structure which reduces the metal density and allows light to pass through [144], [148] (see Fig. 14(a) and (b)), or by employing so-called transparent conducting oxides (TCOs) such as Indium tin oxide (ITO) [149], [150], [151] (see Fig. 14(c)), respectively. Furthermore, a combination of both approaches is feasible for optimal performance [142]. Due to ohmic losses, TCOs are rather suited for the range below 10 GHz, whereas meshed structures are also feasible at mm-wave frequencies, e.g., at 60 GHz [152] or 77 GHz [148]. Above 100 GHz, fabrication of a fine, dense mesh becomes challenging, leading to a trade-off between fabrication effort and achievable transparency.

Glass is an emerging substrate material for mm-wave antennas, not only due to its transparency, but also for its low-loss characteristic and low surface roughness. It can act as carrier material for silicon-on-glass dielectric antennas enabling

FIGURE 15. Antennas based on TGVs. (a) End-fire helix at 58 GHz [153] (b) AiP monopole at 62 GHz [154].
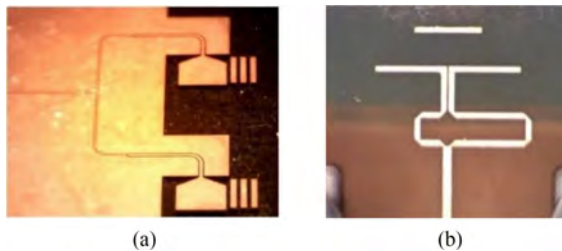
FIGURE 16. Yagi-Uda antennas on 100 μm-thin laminated glass substrate for integration into package. (a) Broadband 2 × 1-element array operating from 24.25 GHz up to 40 GHz [14], (b) AiP connected to IC, realized at 28 GHz [15].

FIGURE 17. Periodic structures. (a) Folded RA at 400 GHz [167], (b) reconfigurable MEMS FSS UC at 30 GHz [172], (c) optically and RF transparent meta-glass at 28 GHz [173].

unconventional shapes, such as a suspended tapered antenna operating between 110 GHz and 130 GHz [106]. Naqvi et al. presented a wideband (50 GHz–65 GHz) micromachined helical end-fire antenna in planar form based on TGVs in borosilicate glass [153], see Fig. 15(a).

More classical is the application of TGVs for antennas integrated into a package, such as the monopole antenna in package (AiP) for chip-to-chip communication [154] depicted in Fig. 15(b). Several planar Yagi-Uda antennas compatible with the glass-polymer package topology (including TGVs) sketched in Fig. 5(a) have already been proposed. Fig. 16(a) shows a (2 × 1)-element array on 100 μm-thin laminated glass substrate, enabling broadband operation between 24.25 GHz and 40 GHz [155]. Watanabe et al. presented a Yagi antenna based on a dipole at 28 GHz, see Fig. 16(b). Integration of this antenna with an IC was proven experimentally as well, including the characterization of the corresponding low-loss interconnects [26]. An extension of this antenna structure to small arrays of up to 4 × 1 elements is shown i [83] Further AiPs based on the same glass-polymer packaging solution with 100 μm core glass have been realized at 53 GHz [156] and in a wideband variant at 140 GHz covering the whole D-band [87]. Apart from that, a compact integrated patch antenna design for radar applications at 77 GHz comprising a stack of five non-laminated glass wafers with TGVs is described in [99]. Other examples of AiPs based on TGVs are holographic leaky-wave antennas, realized at 150 GHz [157] and at 77 GHz for automotive radar systems [158]; in both cases the metal structure is deposited on the glass wafer by PVD. As an alternative to TGVs, Xia et al. proposed a tapered slot antenna for radar sensors at 60 GHz integrated in a flip-chip package [110].
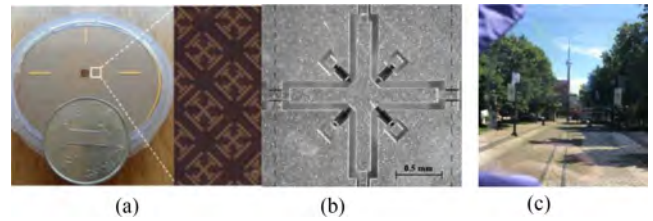
When stacked onto an MMIC as a superstrate, a ca. 100 μm-thin quartz glass layer can improve coupling to free space, as proposed for a radar MMIC in QFN package at 160 GHz [159] and a reconfigurable reflectarray (RA) element at 240 GHz [160]. Such thin quartz superstrates have also been applied in chip-based phased arrays, both for small-scale structures at up to 400 GHz [161] and wafer-scale arrays at 60 GHz, where a 256-element array enables beam steering with a scan angle of up to ±25° [162]. Very recently, wafer-scale phased arrays with quartz superstrates have also become subject of considerable attention in academia and industry for 6G applications at D-band [163], [164], [165]. Moreover, quartz is popular as front and back substrate in reconfigurable arrays based on LC [138] and has been employed in the same manner for RAs as well [166]. Non-reconfigurable RAs on fused silica substrate have been realized even at 400 GHz in the form of a folded RA to create a planar phase front [167], cf. Fig. 17(a). Similarly, a passive transmitarray embedded into laminated car glass has been designed to reduce the penetration loss across a car window by beam shaping and improved matching at 38.5 GHz [168].

Frequency selective surfaces (FSSs) on glass can serve as spatial filters in beam steering scenarios, such as to reduce specular reflections of a carrier substrate, demonstrated at 240 GHz [169]. FSSs usually perform frequency filtering, such as the band stop filter at 27 GHz in [170], which was fabricated by printing silver nanoparticles onto a glass substrate by means of inkjet technology. Commonly, demonstrators up to the THz range are manufactured utilizing conventional photolithography processes [171], where the high surface quality of glass wafers is a key advantage compared with standard circuit board materials, allowing to produce miniaturized structures with high accuracy. To implement tunability, Schoenlinner et al. proposed an FSS with reconfigurable transmission characteristic based on MEMS switches at 30 GHz [172]; the respective unit cell (UC) is depicted in Fig. 17(b).

When optical transparency is essential and propagation or scattering characteristics shall be controlled, transparent metasurfaces are called into action, e.g., when a standard glass window shall feature excellent RF transmission as well. Safari et al. proposed a honeycomb structure with transparent multilayer conductive coatings at 28 GHz [173], achieving about 80% optical and RF transparency, see Fig. 17(c). A

complementary honeycomb structure was embedded into the thin metal oxide coating layer of energy-saving glass to improve indoor outdoor communication at about 2 GHz [174]. To increase the coverage of communication networks indoors, a dynamic metasurface for reflection and transmission control could be attached to building windows; an exemplary design is investigated at 28 GHz [175]. Such metasurfaces, e.g., designed to focus a wave entering a building onto a repeater element or reflector, allow the signal to be amplified and reradiated, resulting in improved indoor signal strength and coverage. Dynamic control of such a metalens enables the deployment of multiple repeaters to switch between users at different locations.

V. CONCLUSION AND OUTLOOK

This article provides a broad overview of current glass technologies for various of RF applications ranging from MHz-to-THz frequencies. Given the high relevance of glass substrate technologies for next-generation RF systems, they are contrasted with conventional material systems highlighting their pros and cons in terms of integration, scalability, and RF performance. Depending on the composition and manufacturing technique, different glass types are discussed with particular focus on their dielectric and thermal properties. This is followed by the review of current key technologies for structuring and metallizing of glass substrates. On package and interposer level, recent developments of glass-enhanced integration solutions are rigorously reported, showing superior I/O densities and RF characteristics. Finally, the increasing popularity of RF glass technologies in both academia and industry is demonstrated by numerous components such as interconnects, filters, resonators, antennas, and quasi-optical structures.

Looking ahead, there are abundant opportunities, where glass can be highly suitable to address the demands of next-generation microelectronic RF systems. While silicon and organic interposers are the most prevalent technologies for high-data-rate HPC systems, glass interposers are expected to have significant market penetration in the upcoming years. For instance, these glass interposers have the potential to provide efficient thermal management through microfluidic cooling technologies on the one side, and high-density high-bandwidth interconnects across multiple chiplets on the other side. Moreover, glass substrates with microfluidic structures open up entirely new possibilities for biomedical devices, such as for (sub-) nanoliter liquid sensing or lab-on-a-chip applications. It's also envisioned that glass-based SOP architectures play a revolutionary role in future wireless communications and sensing systems operating at mm-wave and THz frequencies. Although heterogeneously integrated RF glass packages has made considerable developments, efforts are still required to further improve process maturity and supply-chain readiness. Beyond high-volume consumer electronics markets, RF glass technologies is also paving the way for a radical paradigm shift in designing RF systems with stringent requirements for reliability and robustness, such as in the military or space segment. Finally, emerging electronic-photonic integrated circuits and their optical interconnects offer great potential for extremely high-bandwidth HPC and communications applications for which glass technology are highly suitable.

REFERENCES

[1] W. Hong et al., "The role of millimeter-wave technologies in 5G/6G wireless communications," *IEEE J. Microwaves*, vol. 1, no. 1, pp. 101–122, Jan. 2021.

[2] T. Chaloun et al., "Electronically steerable antennas for future heterogeneous communication networks: Review and perspectives," *IEEE J. Microwaves*, vol. 2, no. 4, pp. 545–581, Oct. 2022.

[3] R. Mahajan et al., "Embedded multi-die interconnect bridge (EMIB) – A high density, high bandwidth packaging interconnect," in *Proc. IEEE 66th Electron. Compon. Technol. Conf.*, 2016, pp. 557–565.

[4] D. Kissinger, G. Kahmen, and R. Weigel, "Millimeter-wave and terahertz transceivers in SiGe BiCMOS technologies," *IEEE Trans. Microw. Theory Techn.*, vol. 69, no. 10, pp. 4541–4560, Oct. 2021.

[5] A. O. Watanabe, M. Ali, S. Y. B. Sayeed, R. R. Tummala, and M. R. Pulugurtha, "A review of 5G front-end systems package integration," *IEEE Trans. Compon., Packag. Manuf. Technol.*, vol. 11, no. 1, pp. 118–133, Jan. 2021.

[6] R. R. Tummala, "SOP: What is it and why? A new microsystem-integration technology paradigm-Moore's law for system integration of miniaturized convergent systems of the next decade," *IEEE Trans. Adv. Packag.*, vol. 27, no. 2, pp. 241–249, May 2004.

[7] K. K. Samanta and I. D. Robertson, "Surfing the millimeter-wave: Multilayer photoimageable technology for high performance SoP components in systems at millimeter-wave and beyond," *IEEE Microw. Mag.*, vol. 17, no. 1, pp. 22–39, Jan. 2016.

[8] A. A. Nawaz, W. T. Khan, and A. C. Ulusoy, "Organically packaged components and modules: Recent advancements for microwave and mm-wave applications," *IEEE Microw. Mag.*, vol. 20, no. 11, pp. 49–72, Nov. 2019.

[9] T. Zwick, F. Boes, B. Göttel, A. Bhutani, and M. Pauli, "Pea-sized mmW transceivers: QFN-based packaging concepts for millimeter-wave transceivers," *IEEE Microw. Mag.*, vol. 18, no. 6, pp. 79–89, Sep./Oct. 2017.

[10] D. G. Kam, D. Liu, A. Natarajan, S. Reynolds, H.-C. Chen, and B. A. Floyd, "LTCC packages with embedded phased-array antennas for 60 GHz communications," *IEEE Microw. Wireless Compon. Lett.*, vol. 21, no. 3, pp. 142–144, Mar. 2011.

[11] X. Gu et al., "Development, implementation, and characterization of a 64-element dual-polarized phased-array antenna module for 28-GHz high-speed data communications," *IEEE Trans. Microw. Theory Techn.*, vol. 67, no. 7, pp. 2975–2984, Jul. 2019.

[12] K. K. W. Low, T. Kanar, S. Zihir, and G. M. Rebeiz, "A 17.7-20.2-GHz 1024-element K-band SATCOM phased-array receiver with 8.1-dB/K G/T, ± 70° beam scanning, and high transmit isolation," *IEEE Trans. Microw. Theory Techn.*, vol. 70, no. 3, pp. 1769–1778, Mar. 2022.

[13] T. G. Lenihan, L. Matthew, and E. J. Vardaman, "Developments in 2.5D: The role of silicon interposers," in *Proc. IEEE 15th Electron. Packag. Technol. Conf.*, 2013, pp. 53–55.

[14] I. Wolff, C. Günner, J. Kassner, R. Kulke, and P. Uhlig, "New heights for satellites: LTCC multilayer technology for future satellites," *IEEE Microw. Mag.*, vol. 19, no. 1, pp. 36–47, Jan./Feb. 2018.

[15] R. Tummala et al., "Glass panel packaging, as the most leading-edge packaging: Technologies and applications," in *Proc. Pan Pacific Microelectron. Symp.*, 2020, pp. 1–5.

[16] K. Oi et al., "Development of new 2.5D package with novel integrated organic interposer substrate with ultra-fine wiring and high density bumps," in *Proc. IEEE 64th Electron. Compon. Technol. Conf.*, 2014, pp. 348–353.

[17] W. J. Lambert et al., "Scalable multichip packaging with integrated antenna array for a 73-GHz transceiver IC," *IEEE Trans. Microw. Theory Techn.*, vol. 69, no. 1, pp. 387–398, Jan. 2021.

[18] K. Zoschke et al., "TSV based silicon interposer technology for wafer level fabrication of 3D SiP modules," in *Proc. IEEE 61st Electron. Compon. Technol. Conf.*, 2011, pp. 836–843.

[19] S. Ravichandran, S. Yamada, F. Liu, V. Smet, M. Kathaperumal, and R. Tummala, "Low-cost non-TSV based 3D packaging using glass panel embedding (GPE) for power-efficient, high-bandwidth heterogeneous integration," in *Proc. IEEE 69th Electron. Compon. Technol. Conf.*, 2019, pp. 1796–1802.

[20] U. Shah, J. Liljeholm, J. Campion, T. Ebefors, and J. Oberhammer, "Low-loss, high-linearity RF interposers enabled by through glass vias," *IEEE Microw. Wireless Compon. Lett.*, vol. 28, no. 11, pp. 960–962, Nov. 2018.

[21] L. Cai et al., "Glass for 5G applications," *Appl. Phys. Lett.*, vol. 119, Aug. 2021, Art. no. 082901.

[22] V. Sukumaran, T. Bandyopadhyay, V. Sundaram, and R. Tummala, "Low-cost thin glass interposers as a superior alternative to silicon and organic interposers for packaging of 3-D ICs," *IEEE Trans. Compon., Packag. Manuf. Technol.*, vol. 2, no. 9, pp. 1426–1433, Sep. 2012.

[23] A. Usman et al., "Interposer technologies for high-performance applications," *IEEE Trans. Compon., Packag. Manuf. Technol.*, vol. 7, no. 6, pp. 819–828, Jun. 2017.

[24] Schott, "Connectors and feedthroughs for security and defense." 2023. Accessed: Feb. 3, 2023. [Online]. Available: https://www.schott.com/en-pl/products/connectors-and-feedthroughs-for-security-and-defense-p1000273

[25] H. Lu et al., "Design, modeling, fabrication and characterization of 2–5-μm redistribution layer traces by advanced semiadditive processes on low-cost panel-based glass interposers," *IEEE Trans. Compon., Packag. Manuf. Technol.*, vol. 6, no. 6, pp. 959–967, Jun. 2016.

[26] A. O. Watanabe et al., "Ultrathin antenna-integrated glass-based millimeter-wave package with through-glass vias," *IEEE Trans. Microw. Theory Techn.*, vol. 68, no. 12, pp. 5082–5092, Dec. 2020.

[27] M. Ali et al., "First demonstration of compact, ultra-thin low-pass and bandpass filters for 5G small-cell applications," *IEEE Microw. Wireless Compon. Lett.*, vol. 28, no. 12, pp. 1110–1112, Dec. 2018.

[28] T. Galler, T. Chaloun, K. Kröhnert, M. Schulz-Ruhtenberg, and C. Waldschmidt, "Hermetically sealed glass package for highly integrated MMICs," in *Proc. Eur. Microw. Conf.*, 2019, pp. 292–295.

[29] T. Kamgaing, A. A. Elsherbini, T. W. Frank, S. N. Oster, and V. R. Rao, "Investigation of a photodefinable glass substrate for millimeter-wave radios on package," in *Proc. IEEE 64th Electron. Compon. Technol. Conf.*, 2014, pp. 1610–1615.

[30] Samtec, "Glass core technology." 2023. Accessed: Feb. 3, 2023. [Online]. Available: https://www.samtec.com/s2s/microelectronics/glass-core-technology

[31] S. Takahashi, Y. Sato, K. Horiuchi, and M. Ono, "Development of high frequency device using glass or fused silica with 3D integration," in *Proc. IEEE 67th Electron. Compon. Technol. Conf.*, 2017, pp. 758–763.

[32] N. Chudpooti et al., "Wideband dielectric properties of silicon and glass substrates for terahertz integrated circuits and microsystems," *Mater. Res. Exp.*, vol. 8, May 2021, Art. no. 056201.

[33] C. A. Harper, *Handbook of Ceramics Glasses, and Diamonds*. New York, NY, USA: McGraw-Hill, 2001.

[34] M. Letz, "Glasses and glass ceramics for applications in high frequency electronics," in *Proc. IEEE MTT-S Int. Microw. Workshop Ser. Adv. Mater. Processes RF THz Appl.*, 2019, pp. 85–87.

[35] H. Namikawa, "Characterization of the diffusion process in oxide glasses based on the correlation between electric conduction and dielectric relaxation," *J. Non-Crystalline Solids*, vol. 18, pp. 173–195, Sep. 1975.

[36] Schott, "SCHOTT D 263 borosilicate glass," 2023. Accessed: Jan. 25, 2023. [Online]. Available: https://www.schott.com/de-de/products/d-263-p1000318

[37] Schott, "SCHOTT MEMpax borosilicate glass." 2023. Accessed: Jan. 25, 2023. [Online]. Available: https://www.schott.com/en-us/products/mempax-p1000322

[38] Schott, "SCHOTT AF 32 eco." 2023. Accessed: Jan. 25, 2023. [Online]. Available: https://www.schott.com/en-us/products/af-32-eco-p1000308

[39] W. Höland, *Glass-Ceramic Technology*, 3rd ed. Hoboken, NJ, USA: Wiley, 2012.

[40] T. Okamura and T. Kishino, "Dielectric properties of rare-earth-added cordierite at microwave and millimeter wave frequencies," *Jpn. J. Appl. Phys.*, vol. 37, Sep. 1998, Art. no. 5364.

[41] J. W. Lamb, "Miscellaneous data on materials for millimetre and submillimetre optics," *Int. J. Infrared Millimeter Waves*, vol. 17, pp. 1997–2034, Dec. 1996.

[42] Schott, "SCHOTT BOROFLOAT floated borosilicate glass." 2023. Accessed: Jan. 25, 2023. [Online]. Available: https://www.schott.com/en-us/products/borofloat-p1000314

[43] S. Musikant, "Glass," in *Encyclopedia of Physical Science and Technology*, R. A. Meyers, Ed., 3rd ed. New York, NY, USA: Academic, 2003, pp. 781–806.

[44] Skyworks, "D-4 cordierite," 2023. [Online]. Available: https://www.skyworksinc.com/en/Products/Technical-Ceramics/D-4-Cordierite

[45] Rogers Corporation, "Rogers RO3003 high frequency laminates," Jan. 2023. [Online]. Available: https://www.rogerscorp.com/advanced-electronics-solutions/ro3000-series-laminates/ro3003-laminates

[46] Panasonic Industry Co., Ltd., "MEGTRON7 - Ultra-low transmission loss highly heat resistant multi-layer circuit board materials," 2023. Accessed: Jan. 30, 2023. [Online]. Available: https://industrial.panasonic.com/ww/products/pt/megtron/megtron7

[47] Ferro Corporation, "A6M-E LTCC material systems for high-frequency applications," Jan. 2023. Accessed: Jan. 30, 2023. [Online]. Available: https://www.ferro.com/products/product-category/electronic-materials/ltcc-material-systems/low-temperature-co-fired-_ltcc_--materials/a6m-e-ltcc-material-systems-for-high-frequency-applications

[48] R. Ostholt, N. Ambrosius, and R. A. Kruger, "High speed through glass via manufacturing technology for interposer," in *Proc. 5th Electron. Syst.-Integration Technol. Conf.*, 2014, pp. 1–3.

[49] R. Ostholt, N. Ambrosius, D. Dunker, and J.-P. Delrue, "High-throughput via formation in solid-core glass for IC substrates," in *Proc. MiNaPAD Conf.*, 2017, pp. 1–3.

[50] T. Galler et al., "Glass package for radar MMICs above 150 GHz," *IEEE J. Microwaves*, vol. 2, no. 1, pp. 97–107, Jan. 2022.

[51] R. Santos, N. Anspach, N. Ambrosius, S. Schmidt, and R. Ostholt, "Fabrication of panel-level glass substrates with complete design freedom using LIDE," in *Proc. Int. Symp. Microelectron.*, 2022, pp. 1–3.

[52] H. Moriceau et al., "Overview of recent direct wafer bonding advances and applications," *Adv. Natural Sci., Nanosci. Nanotechnol.*, vol. 1, pp. 1–11, Feb. 2011.

[53] M. A. Schmidt, "Wafer-to-wafer bonding for microstructure formation," *Proc. IEEE*, vol. 86, no. 8, pp. 1575–1585, Aug. 1998.

[54] EV Group, "Solutions for MEMS," Jan. 2022. [Online]. Available: https://www.evgroup.com/fileadmin/media/technologies/EVG_Solutions_for_MEMS_Brochure_22_01.pdf

[55] A. Berthold, L. Nicola, P. M. Sarro, and M. J. Vellekoop, "Glass-to-glass anodic bonding with standard IC technology thin films as intermediate layers," *Sensors Actuators A, Phys.*, vol. 82, pp. 224–228, May 2000.

[56] L. A. Hof and J. Abou Ziki, "Micro-hole drilling on glass substrates—A review," *Micromachines*, vol. 8, pp. 1–23, Feb. 2017.

[57] D. Li, Z. Shang, Y. She, and Z. Wen, "Investigation of Au/Si eutectic wafer bonding for MEMS accelerometers," *Micromachines*, vol. 8, pp. 1–12, May 2017.

[58] E. Kaiser, "Laser welding of glass replaces glueing procedure," *Laser Technik J.*, vol. 13, pp. 22–25, 2016.

[59] A. M. Zawacka, M. S. Prediger, A. Kassner, F. Dencker, and M. C. Wurz, "Approaches for a solely electroless metallization of through-glass vias," in *Proc. IEEE 72nd Electron. Compon. Technol. Conf.*, 2022, pp. 889–897.

[60] M. J. Laakso et al., "Through-glass vias for glass interposers and MEMS packaging applications fabricated using magnetic assembly of microscale metal wires," *IEEE Access*, vol. 6, pp. 44306–44317, 2018.

[61] A. B. Shorey and R. Lu, "Progress and application of through glass via (TGV) technology," in *Proc. Pan Pacific Microelectron. Symp.*, 2016, pp. 1–6.

[62] M. Töpper et al., "3-D thin film interposer based on TGV (Through glass vias): An alternative to Si-interposer," in *Proc. 60th Electron. Compon. Technol. Conf.*, 2010, pp. 66–73.

[63] Y. Ohara, Y. Inagaki, M. Matsui, and K. Asami, "A cost effective via last TSV technology using molten solder filling for automobile application," in *Proc. IEEE 67th Electron. Compon. Technol. Conf.*, 2017, pp. 47–52.

[64] E. Liew et al., "Signal transmission loss due to copper surface roughness in high-frequency region," presented at IPC APEX EXPO 2014: New Ideas... For New Horizons, 2014, pp. 1–16.

[65] K. Kröhnert et al., "High aspect ratio through-glass vias as heat conductive element," in *Proc. IMAPS Nordic Conf. Microelectron. Packag.*, 2022, pp. 1–6.

[66] S. Takahashi et al., "Development of through glass via technology for 3D packaging," in *Proc. Eur. Microelectron. Packag. Conf.*, 2013, pp. 1–4.

[67] S. Onitake, K. Inoue, M. Takayama, T. Kozuka, S. Kuramochi, and H. Yun, "TGV (thru-glass via) metallization by direct Cu plating on glass," in *Proc. IEEE 66th Electron. Compon. Technol. Conf.*, 2016, pp. 1316–1321.

[68] Y. Wang, S. Ma, X. Liu, and J. Zhao, "Partially filled TGV based on double sides Cu conformal electroplating process for MEMS vacuum packaging," in *Proc. Int. Conf. Electron. Packag.*, 2022, pp. 53–54.

[69] A. B. Shorey, S. F. Nelson, D. Levy, and P. Ballentine, "Glass solutions for wafer level packaging," in *Proc. Int. Wafer Level Packag. Conf.*, 2019, pp. 1–6.

[70] J. H. Lau, "Recent advances and trends in advanced packaging," *IEEE Trans. Compon., Packag. Manuf. Technol.*, vol. 12, no. 2, pp. 228–252, Feb. 2022.

[71] T. Sowlati et al., "A 60-GHz 144-element phased-array transceiver for backhaul application," *IEEE J. Solid-State Circuits*, vol. 53, no. 12, pp. 3640–3659, Dec. 2018.

[72] D. G. Kam, D. Liu, A. Natarajan, S. K. Reynolds, and B. A. Floyd, "Organic packages with embedded phased-array antennas for 60-GHz wireless chipsets," *IEEE Trans. Compon., Packag. Manuf. Technol.*, vol. 1, no. 11, pp. 1806–1814, Nov. 2011.

[73] C.-C. Lee et al., "An overview of the development of a GPU with integrated HBM on silicon interposer," in *Proc. IEEE 66th Electron. Compon. Technol. Conf.*, 2016, pp. 1439–1444.

[74] M. Wojnowski, C. Wagner, R. Lachner, J. Böck, G. Sommer, and K. Pressel, "A 77-GHz SiGe single-chip four-channel transceiver module with integrated antennas in embedded wafer-level BGA package," in *Proc. IEEE 62nd Electron. Compon. Technol. Conf.*, 2012, pp. 1027–1032.

[75] A. Hagelauer, M. Wojnowski, K. Pressel, R. Weigel, and D. Kissinger, "Integrated systems-in-package: Heterogeneous integration of millimeter-wave active circuits and passives in fan-out wafer-level packaging technologies," *IEEE Microw. Mag.*, vol. 19, no. 1, pp. 48–56, Jan./Feb. 2018.

[76] W.-W. Shen et al., "Ultrathin glass wafer lamination and laser debonding to enable glass interposer fabrication," in *Proc. IEEE 65th Electron. Compon. Technol. Conf.*, 2015, pp. 1652–1657.

[77] K. Demir, T. Ogawa, V. Sundaram, P. M. Raj, and R. R. Tummala, "Reliability of through-package-vias from via-first processing with ultra-thin glass," *IEEE Trans. Device Mater. Rel.*, vol. 17, no. 4, pp. 683–691, Dec. 2017.

[78] H. Cai et al., "Design, fabrication, and radio frequency property evaluation of a through-glass-via interposer for 2.5D radio frequency integration," *J. Micromechanics Microeng.*, vol. 29, May 2019, Art. no. 075002.

[79] S. Ravichandran et al., "2.5D glass panel embedded (GPE) packages with better I/O density, performance, cost and reliability than current silicon interposers and high-density fan-out packages," in *Proc. IEEE 68th Electron. Compon. Technol. Conf.*, 2018, pp. 625–630.

[80] S. Ravichandran, M. Kathaperumal, M. Swaminathan, and R. Tummala, "Large-body-sized glass-based active interposer for high-performance computing," in *Proc. IEEE 70th Electron. Compon. Technol. Conf.*, 2020, pp. 879–884.

[81] S. Ravichandran, V. Smet, M. Swaminathan, and R. Tummala, "Demonstration of glass-based 3D package architectures with embedded dies for high performance computing," in *Proc. IEEE 72nd Electron. Compon. Technol. Conf.*, 2022, pp. 1114–1120.

[82] T. Shi et al., "First demonstration of panel glass fan-out (GFO) packages for high I/O density and high frequency multi-chip integration," in *Proc. IEEE 67th Electron. Compon. Technol. Conf.*, 2017, pp. 41–46.

[83] M. Ali et al., "Package-integrated, wideband power dividing networks and antenna arrays for 28-GHz 5G new radio bands," *IEEE Trans. Compon., Packag. Manuf. Technol.*, vol. 10, no. 9, pp. 1515–1523, Sep. 2020.

[84] T. Yu, X. Zhang, L. Chen, X. Ren, Z. Duan, and D. Yu, "Development of embedded glass wafer fan-out package with 2D antenna arrays for 77GHz millimeter-wave chip," in *Proc. IEEE 70th Electron. Compon. Technol. Conf.*, 2020, pp. 31–36.

[85] A. O. Watanabe et al., "Glass-based IC-embedded antenna-integrated packages for 28-GHz high-speed data communications," in *Proc. IEEE 70th Electron. Compon. Technol. Conf.*, 2020, pp. 89–94.

[86] T. Shi, Y. Gong, S. Ravichandran, V. Sundaram, J. D. Cressler, and R. Tummala, "Next generation of automotive radar with leading-edge advances in SiGe devices and glass panel embedding (GPE)," in *Proc. IEEE 68th Electron. Compon. Technol. Conf.*, 2018, pp. 1245–1250.

[87] S. Erdogan and M. Swaminathan, "D-band Quasi-Yagi antenna in glass-based package," in *Proc. IEEE MTT-S Int. Microw. RF Conf.*, 2021, pp. 1–4.

[88] X. Jia et al., "Antenna-integrated, die-embedded glass package for 6G wireless applications," in *Proc. IEEE 72nd Electron. Compon. Technol. Conf.*, 2022, pp. 377–383.

[89] F. Liu et al., "Innovative Sub-5- μ m microvias by picosecond UV laser for post-moore packaging interconnects," *IEEE Trans. Compon., Packag. Manuf. Technol.*, vol. 9, no. 10, pp. 2016–2023, Oct. 2019.

[90] B. Sadhu, X. Gu, and A. Valdes-Garcia, "The more (antennas), the merrier: A survey of silicon-based mm-wave phased arrays using multi-IC scaling," *IEEE Microw. Mag.*, vol. 20, no. 12, pp. 32–50, Dec. 2019.

[91] D. Yu, Z. Huang, Z. Xiao, L. Yang, and M. Xiang, "Embedded Si fan out: A low cost wafer level packaging technology without molding and de-bonding processes," in *Proc. IEEE 67th Electron. Compon. Technol. Conf.*, 2017, pp. 28–34.

[92] P. H. Wang, Y. C. Lee, C. K. Lee, H. H. Chang, and K. N. Chiang, "Solder joint reliability assessment and pad size studies of FO-WLP with glass substrate," *IEEE Trans. Device Mater. Rel.*, vol. 21, no. 1, pp. 96–101, Mar. 2021.

[93] T. Galler et al., "MMIC-to-dielectric waveguide transitions for glass packages above 150 GHz," *IEEE Trans. Microw. Theory Techn.*, early access, 24 Jan. 2023, doi: 10.1109/TMTT.2023.3236787.

[94] L. Martin et al., "Attenuation of high frequency signals in structured metallization on glass: Comparing different metallization techniques with 24 GHz, 77 GHz and 100 GHz structures," in *Proc. IEEE 69th Electron. Compon. Technol. Conf.*, 2019, pp. 726–732.

[95] M. U. Rehman, S. Ravichandran, S. Erdogan, and M. Swaminathan, "W-band and D-band transmission lines on glass based substrates for sub-THz modules," in *Proc. IEEE 70th Electron. Compon. Technol. Conf.*, 2020, pp. 660–665.

[96] T. Yu, K. Xue, K. Li, Y. Liang, and D. Yu, "Characteristics of 10–110GHz transmission lines on fused silica substrate for millimeter-wave modules," in *Proc. Int. Conf. Electron. Packag. Technol.*, 2021, pp. 1–5.

[97] A. O. Watanabe et al., "First demonstration of 28 GHz and 39 GHz transmission lines and antennas on glass substrates for 5G modules," in *Proc. IEEE 67th Electron. Compon. Technol. Conf.*, 2017, pp. 236–241.

[98] X. Jia and M. Swaminathan, "Integrated low-loss planar goubau lines on glass interposer for 6G wireless applications," in *Proc. IEEE/MTT-S Int. Microw. Symp.*, 2022, pp. 367–370.

[99] Y. Su, D. Yu, W. Ruan, and N. Jia, "Development of compact millimeter-wave antenna by stacking of five glass wafers with through glass vias," *IEEE Electron Device Lett.*, vol. 43, no. 6, pp. 934–937, Jun. 2022.

[100] T. Iwai et al., "Multilayer glass substrate with high density via structure for all inorganic multi-chip module," in *Proc. IEEE 69th Electron. Compon. Technol. Conf.*, 2019, pp. 1952–1957.

[101] M. ur Rehman, A. Watanabe, S. Ravichandran, and M. Swaminathan, "Substrate integrated waveguides in glass interposers for mm wave applications," in *Proc. IEEE MTT-S Int. Microw. Symp.*, 2021, pp. 339–341.

[102] I.-J. Hyeon and C.-W. Baek, "Micromachined substrate integrated waveguides with electroplated copper vias in reflowed glass substrate for millimeter-wave applications," *Microelectron. Eng.*, vol. 131, pp. 1–23, Jan. 2015.

[103] M. Geiger, M. Hitzler, S. Saulig, J. Iberle, P. Hügler, and C. Waldschmidt, "A 160-GHz radar with flexible antenna used as a sniffer probe," *IEEE Sensor J.*, vol. 17, no. 16, pp. 5104–5111, Aug. 2017.

[104] J. Weinzierl, C. Fluhrer, and H. Brand, "Dielectric waveguides at sub-millimeter wavelengths," in *Proc. IEEE 6th Int. Conf. THz Electron.*, 1998, pp. 166–169.

[105] T. Galler, M. Schulz-Ruhtenberg, T. Chaloun, and C. Waldschmidt, "Mechanically flexible dielectric waveguides and bandstop filters in glass technology at G-band," in *Proc. Eur. Microw. Conf.*, 2022, pp. 294–297.

[106] N. Ranjkesh, M. Basha, A. Taeb, A. Zandieh, S. Gigoyan, and S. Safavi-Naeini, "Silicon-on-glass dielectric waveguide—Part I: For millimeter-wave integrated circuits," *IEEE Trans. THz Sci. Technol.*, vol. 5, no. 2, pp. 268–279, Mar. 2015.

[107] N. Ranjkesh, M. Basha, A. Taeb, and S. Safavi-Naeini, "Silicon-on-glass dielectric waveguide—Part II: For THz applications," *IEEE Trans. THz Sci. Technol.*, vol. 5, no. 2, pp. 280–287, Mar. 2015.

[108] N. Ranjkesh, S. Gigoyan, H. Amarloo, M. Basha, and S. Safavi-Naeini, "Broadband single-mode THz suspended silicon-on-glass waveguide," *IEEE Microw. Wireless Compon. Lett.*, vol. 28, no. 3, pp. 185–187, Mar. 2018.

[109] T. V. Dinh et al., "Bonding-wire-geometric-profile-dependent model for mutual coupling between two bonding wires on a glass substrate," *IEEE Trans. Compon., Packag. Manuf. Technol.*, vol. 5, no. 1, pp. 119–127, Jan. 2015.

[110] H. Xia, T. Zhang, L. Li, and F.-C. Zheng, "A 1 × 2 taper slot antenna array with flip-chip interconnect via glass-IPD technology for 60 GHz radar sensors," *IEEE Access*, vol. 8, pp. 61790–61796, 2020.

[111] K. Kröhnert et al., "Versatile hermetically sealed sensor platform for high frequency applications," in *Proc. Eur. Microelectron. Packag. Conf.*, 2021, pp. 1–8.

[112] M. Hitzler, S. Saulig, L. Boehm, W. Mayer, and C. Waldschmidt, "MMIC-to-waveguide transition at 160 GHz with galvanic isolation," in *Proc. IEEE MTT-S Int. Microw. Symp.*, 2016, pp. 1–4.

[113] Z. Gao, M. Tang, P. Gao, H. Yue, and Y. Tang, "Design and measurement of D-band bonding-wire interconnection on quartz glass substrate," in *Proc. Int. Conf. Microw. Millimeter Wave Technol.*, 2020, pp. 1–3.

[114] A. O. Watanabe, H. Ito, R. P. Markondeya, R. R. Tummala, and M. Swaminathan, "Low-loss impedance-matched sub-25-μm vias in 3-D millimeter-wave packages," *IEEE Trans. Compon., Packag. Manuf. Technol.*, vol. 10, no. 5, pp. 870–877, May 2020.

[115] S. Erdogan, S. Ravichandran, X. Jia, and M. Swaminathan, "Characterization of chip-to-package interconnects for glass panel embedding (GPE) for sub-THz wireless communications," in *Proc. IEEE 71st Electron. Compon. Technol. Conf.*, 2021, pp. 2328–2333.

[116] A. O. Watanabe, K. Kanno, H. Ito, R. R. Tummala, and M. Swaminathan, "High-density low-loss millimeter-wave package interconnects with the impact of dielectric-material surface roughness," *Appl. Phys. Lett.*, vol. 119, Sep. 2021, Art. no. 134103.

[117] M. Ali, K.-Q. Huang, M. Swaminathan, P. M. Raj, and R. R. Tummala, "Laminated glass-based, compact inline stepped-impedance resonator bandpass filters for 5G new radio modules," *IEEE Trans. Compon., Packag. Manuf. Technol.*, vol. 11, no. 4, pp. 708–711, Apr. 2021.

[118] A. Maestrini et al., "Schottky diode-based terahertz frequency multipliers and mixers," *Comptes Rendus Physique*, vol. 11, pp. 480–495, Aug. 2010.

[119] Z. Chen, B. Zhang, Y. Zhang, G. Yue, Y. Fan, and Y. Yuan, "220 GHz outdoor wireless communication system based on a Schottky-diode transceiver," *IEICE Electron. Exp.*, vol. 13, 2016, Art. no. 20160282.

[120] J. Meng, D. Zhang, G. Ji, C. Yao, C. Jiang, and S. Liu, "Design of a 335 GHz frequency multiplier source based on two schemes," *Electronics*, vol. 8, pp. 1–12, Aug. 2019.

[121] G. Ji, D. Zhang, J. Meng, S. Liu, and C. Yao, "Design and measurement of a 0.67 THz biased sub-harmonic mixer," *Electronics*, vol. 9, pp. 1–11, Jan. 2020.

[122] S. Yang, M. Xu, X. Jia, and W. Jiang, "Multilayer SIW filter for advanced packaging based on glass substrates," in *Proc. IEEE MTT-S Int. Wireless Symp.*, 2020, pp. 1–3.

[123] D. Psychogiou and A. Ashley, "Glass-based bandpass filters for new radio (NR) K-/Ka-band communications," *IEEE Trans. Compon., Packag. Manuf. Technol.*, vol. 12, no. 5, pp. 887–889, May 2022.

[124] M. Tanaka et al., "Experimental study of through glass via effects on high frequency electrical characteristics," in *Proc. Int. Conf. Electron. Packag.*, 2018, pp. 184–188.

[125] C. Zhang, A. Cocking, E. Freeman, Z. Liu, and S. Tadigadapa, "On-chip glass microspherical shell whispering gallery mode resonators," *Sci. Rep.*, vol. 7, pp. 1–11, Nov. 2017.

[126] E. N. Shaforost, N. Klein, S. A. Vitusevich, A. Offenhäusser, and A. A. Barannik, "Nanoliter liquid characterization by open whispering-gallery mode dielectric resonators at millimeter wave frequencies," *J. Appl. Phys.*, vol. 104, 2008, Art. no. 074111.

[127] E. Freeman et al., "Novel chip-scale high-Q whispering gallery mode resonator as a magnetometer," in *Proc. IEEE SENSORS*, 2017, pp. 1–3.

[128] K. W. Leung, E. H. Lim, and X. S. Fang, "Dielectric resonator antennas: From the basic to the aesthetic," *Proc. IEEE*, vol. 100, no. 7, pp. 2181–2193, Jul. 2012.

[129] K. W. Leung, X. S. Fang, Y. M. Pan, E. H. Lim, K. M. Luk, and H. P. Chan, "Dual-function radiating glass for antennas and light covers—Part II: Dual-band glass dielectric resonator antennas," *IEEE Trans. Antennas Propag.*, vol. 61, no. 2, pp. 587–597, Feb. 2013.

[130] Z. Chen, H. Wong, and J. Kelly, "A polarization-reconfigurable glass dielectric resonator antenna using liquid metal," *IEEE Trans. Antennas Propag.*, vol. 67, no. 5, pp. 3427–3432, May 2019.

[131] C. Bartlett, A. Malavé, M. Letz, and M. Höft, "Structured-glass waveguide technology for high-performance millimetre-wave components and systems," *IEEE J. Microwaves*, vol. 2, no. 2, pp. 307–315, Apr. 2022.

[132] L. Martoglio, E. Richalot, G. Lissorgues-Bazin, and O. Picon, "Low-cost inverted line in silicon/glass technology for filter in the Ka-band," *IEEE Trans. Microw. Theory Techn.*, vol. 54, no. 7, pp. 3084–3089, Jul. 2006.

[133] T. Seki, "Recent progress in packaging of RF MEMS," in *Proc. IEEE Compound Semicond. Integr. Circuit Symp.*, 2004, pp. 233–236.

[134] J.-Y. Lee, S.-W. Lee, S.-K. Lee, and J.-H. Park, "Through-glass copper via using the glass reflow and seedless electroplating processes for wafer-level RF MEMS packaging," *J. Micromechanics Microeng.*, vol. 23, Jun. 2013, Art. no. 085012.

[135] T. Markovic, I. Ocket, A. Baric, and B. Nauwelaers, "Design and comparison of resonant and non-resonant single-layer microwave heaters for continuous flow microfluidics in silicon-glass technology," *Energies*, vol. 13, pp. 1–13, May 2020.

[136] L. Jasińska and K. Malecha, "Microfluidic modules integrated with microwave components—Overview of applications from the perspective of different manufacturing technologies," *Sensors*, vol. 21. pp. 1–24, Mar. 2021.

[137] H. Maune, M. Jost, R. Reese, E. Polat, M. Nickel, and R. Jakoby, "Microwave liquid crystal technology," *Crystals*, vol. 8, pp. 1–27, Sep. 2018.

[138] O. H. Karabey, A. Gaebler, S. Strunck, and R. Jakoby, "A 2-D electronically steered phased-array antenna with 2 × 2 elements in LC display technology," *IEEE Trans. Microw. Theory Techn.*, vol. 60, no. 5, pp. 1297–1306, May 2012.

[139] M. Roig, M. Maasch, C. Damm, and R. Jakoby, "Liquid crystal-based tunable CRLH-transmission line for leaky wave antenna applications at Ka-Band," *Int. J. Microw. Wireless Technol.*, vol. 6, pp. 325–330, Jun. 2014.

[140] M. Roig, M. Maasch, C. Damm, and R. Jakoby, "Dynamic beam steering properties of an electrically tuned liquid crystal based CRLH leaky wave antenna," in *Proc. 8th Int. Congr. Adv. Electromagn. Mater. Microw. Opt.*, 2014, pp. 253–255.

[141] X. Liu et al., "Transparent and nontransparent microstrip antennas on a CubeSat: Novel low-profile antennas for CubeSats improve mission reliability," *IEEE Antennas Propag. Mag.*, vol. 59, no. 2, pp. 59–68, Apr. 2017.

[142] B. Xi, X. Liang, Q. Chen, K. Wang, J. Geng, and R. Jin, "Optical transparent antenna array integrated with solar cell," *IEEE Antennas Wireless Propag. Lett.*, vol. 19, no. 3, pp. 457–461, Mar. 2020.

[143] S. Hong, S. H. Kang, Y. Kim, and C. W. Jung, "Transparent and flexible antenna for wearable glasses applications," *IEEE Trans. Antennas Propag.*, vol. 64, no. 7, pp. 2797–2804, Jul. 2016.

[144] J. P. Lombardi et al., "Copper transparent antennas on flexible glass by subtractive and semi-additive fabrication for automotive applications," in *Proc. IEEE 68th Electron. Compon. Technol. Conf.*, 2018, pp. 2107–2115.

[145] Y.-X. Sun, D. Wu, X. S. Fang, and J. Ren, "On-glass grid structure and its application in highly-transparent antenna for internet of vehicles," *IEEE Trans. Veh. Technol.*, vol. 72, no. 1, pp. 93–101, Jan. 2023.

[146] R. B. Green et al., "Optically transparent antennas and filters: A smart city concept to alleviate infrastructure and network capacity challenges," *IEEE Antennas Propag. Mag.*, vol. 61, no. 3, pp. 37–47, Jun. 2019.

[147] G. I. Kiani, L. G. Olsson, A. Karlsson, K. P. Esselle, and M. Nilsson, "Cross-dipole bandpass frequency selective surface for energy-saving glass used in buildings," *IEEE Trans. Antennas Propag.*, vol. 59, no. 2, pp. 520–525, Feb. 2011.

[148] P. Hügler, M. Zaky, M. Roos, S. Strehle, and C. Waldschmidt, "Optically transparent patch antennas at 77 GHz using meshed aluminum," in *Proc. German Microw. Conf.*, 2019, pp. 186–189.

[149] N. Neveu, M. Garcia, J. Casana, R. Dettloff, D. R. Jackson, and J. Chen, "Transparent microstrip antennas for CubeSat applications," in *Proc. IEEE Int. Conf. Wireless Space Extreme Environ.*, 2013, pp. 1–4.

[150] Z. J. Silva, C. R. Valenta, and G. D. Durgin, "Optically transparent antennas: A survey of transparent microwave conductor performance and applications," *IEEE Antennas Propag. Mag.*, vol. 63, no. 1, pp. 27–39, Feb. 2021.

[151] M. D. Poliks et al., "Transparent antennas for wireless systems based on patterned indium tin oxide and flexible glass," in *Proc. IEEE 67th Electron. Compon. Technol. Conf.*, 2017, pp. 1443–1448.

[152] J. Hautcoeur, L. Talbi, and K. Hettak, "Feasibility study of optically transparent CPW-fed monopole antenna at 60-GHz ISM bands," *IEEE Trans. Antennas Propag.*, vol. 61, no. 4, pp. 1651–1657, Apr. 2013.

[153] A. H. Naqvi, J.-H. Park, C.-W. Baek, and S. Lim, "V-band end-fire radiating planar micromachined helical antenna using through-glass silicon via (TGSV) Technology," *IEEE Access*, vol. 7, pp. 87907–87915, 2019.

[154] S. Hwangbo, Y.-K. Yoon, and A. B. Shorey, "Millimeter-wave wireless chip-to-chip (C2C) communications in 3D system-in-packaging (SiP) using compact through glass via (TGV)-integrated antennas," in *Proc. IEEE 68th Electron. Compon. Technol. Conf.*, 2018, pp. 2074–2079.

[155] T.-H. Lin et al., "Broadband and miniaturized antenna-in-package (AiP) design for 5G applications," *IEEE Antennas Wireless Propag. Lett.*, vol. 19, no. 11, pp. 1963–1967, Nov. 2020.

[156] W. T. Khan et al., "A V-band end-fire Yagi-Uda antenna on an ultra-thin glass packaging technology," in *Proc. Eur. Microw. Conf.*, 2015, pp. 618–621.

[157] T. Galler, T. Frey, C. Waldschmidt, and T. Chaloun, "High-gain millimeter-wave holographic antenna in package using glass technology," *IEEE Antennas Wireless Propag. Lett.*, vol. 19, no. 12, pp. 2067–2071, Dec. 2020.

[158] T. Frey, A. Dürr, C. Waldschmidt, and T. Chaloun, "Holographic conical beam scanning antenna for mm-wave radars using glass technology," in *Proc. Eur. Microw. Conf.*, 2022, pp. 825–828.

[159] M. Hitzler, L. Boehm, W. Mayer, and C. Waldschmidt, "Radiation pattern optimization for QFN packages with on-chip antennas at 160 GHz," *IEEE Trans. Antennas Propag.*, vol. 66, no. 9, pp. 4552–4562, Sep. 2018.

[160] S. Brandl et al., "Characterization techniques for reconfigurable reflectarray unit cells at 240 GHz," *IEEE Antennas Wireless Propag. Lett.*, vol. 21, no. 9, pp. 1911–1915, Sep. 2022.

[161] G. M. Rebeiz et al., "Wafer-scale millimeter-wave phased-array RFICs," in *Proc. IEEE Compound Semicond. Integr. Circuit Symp.*, 2014, pp. 1–4.

[162] S. Zihir, O. D. Gurbuz, A. Kar-Roy, S. Raman, and G. M. Rebeiz, "60-GHz 64- and 256-elements wafer-scale phased-array transmitters using full-reticle and subreticle stitching techniques," *IEEE Trans. Microw. Theory Techn.*, vol. 64, no. 12, pp. 4701–4719, Dec. 2016.

[163] S. Li, Z. Zhang, B. Rupakula, and G. M. Rebeiz, "An Eight-Element 140 GHz wafer-scale phased-array transmitter with 32 dBm peak EIRP and >16 Gbps 16QAM and 64QAM operation," in *Proc. IEEE MTT-S Int. Microw. Symp.*, 2021, pp. 795–798.

[164] S. Li, Z. Zhang, B. Rupakula, and G. M. Rebeiz, "An eight-element 140-GHz wafer-scale IF beamforming phased-array receiver with 64-QAM operation in CMOS RFSOI," *IEEE J. Solid-State Circuits*, vol. 57, no. 2, pp. 385–399, Feb. 2022.

[165] M. Elkhouly et al., "Fully integrated 2D scalable TX/RX chipset for D-band phased-array-on-glass modules," in *Proc. IEEE Int. Solid-State Circuits Conf.*, 2022, pp. 76–78.

[166] R. Cahill et al., "Recent progress in electronically tunable reflectarray technology using liquid crystals," in *Proc. Eur. Conf. Antennas Propag.*, 2011, pp. 2866–2870.

[167] Z.-W. Miao, Z.-C. Hao, Y. Wang, B.-B. Jin, J.-B. Wu, and W. Hong, "A 400-GHz high-gain quartz-based single layered folded reflectarray antenna for terahertz applications," *IEEE Trans. THz Sci. Technol.*, vol. 9, no. 1, pp. 78–88, Jan. 2019.

[168] S. Hong, Y. Kim, and J. Oh, "Automobile laminated glass window embedded transmitarray and ray tracing validation for enhanced 5G connectivity," *IEEE Trans. Antennas Propag.*, vol. 70, no. 8, pp. 6671–6682, Aug. 2022.

[169] S. Brandl, A. Diepolder, M. Mueh, C. Damm, and C. Waldschmidt, "Frequency selective surfaces for reduced specular reflection under oblique incidence at 240 GHz," in *Proc. Eur. Conf. Antennas Propag.*, 2023, pp. 1–5.

[170] A. Shastri et al., "3D printing of millimetre wave and low-terahertz frequency selective surfaces using aerosol jet technology," *IEEE Access*, vol. 8, pp. 177341–177350, 2020.

[171] S. Vegesna, Y. Zhu, A. Bernussi, and M. Saed, "Terahertz two-layer frequency selective surfaces with improved transmission characteristics," *IEEE Trans. THz Sci. Technol.*, vol. 2, no. 4, pp. 441–448, Jul. 2012.

[172] B. Schoenlinner, A. Abbaspour-Tamijani, L. C. Kempel, and G. M. Rebeiz, "Switchable low-loss RF MEMS Ka-band frequency-selective surface," *IEEE Trans. Microw. Theory Techn.*, vol. 52, no. 11, pp. 2474–2481, Nov. 2004.

[173] M. Safari, Y. He, M. Kim, N. P. Kherani, and G. V. Eleftheriades, "Optically and radio frequency (RF) transparent meta-glass," *Nanophotonics*, vol. 9, pp. 3889–3898, Jun. 2020.

[174] M. Gustafsson, A. Karlsson, A. P. P. Rebelo, and B. Widenberg, "Design of frequency selective windows for improved indoor outdoor communication," *IEEE Trans. Antennas Propag.*, vol. 54, no. 6, pp. 1897–1900, Jun. 2006.

[175] D. Kitayama, Y. Hama, K. Goto, K. Miyachi, T. Motegi, and O. Kagaya, "Transparent dynamic metasurface for a visually unaffected reconfigurable intelligent surface: Controlling transmission/reflection and making a window into an RF lens," *Opt. Exp.*, vol. 29, pp. 29292–29307, 2021.

[176] R. Santos, N. Ambrosius, R. Ostholt, and J.-P. Delrue, "Bringing new life to glass for wafer-level packaging applications," in *Proc. Int. Wafer Level Packag. Conf.*, 2020, pp. 1–7.

TOBIAS CHALOUN (Member, IEEE) received the Dipl.-Ing. and Dr.-Ing. degrees (with Hons.) in electrical engineering from the University of Ulm, Ulm, Germany, in 2010 and 2016, respectively. From 2010 to 2016, he was a Research Assistant with the Institute of Microwave Engineering, Ulm University, where he conducted his doctoral studies in the field of highly-integrated antenna systems for communication applications at millimeter wave frequencies. Since January 2017, he has been a Senior Researcher and Lecturer with the Institute of Microwave Engineering. His main research interests include multilayer antennas and circuits, millimeter-wave packaging and interconnects, phased array antenna systems, and millimeter-wave radar sensors. He is a Member of the European Microwave Association. He is also a Founding Member of the IEEE MTT-S Technical Committee 29 on Microwave Aerospace Systems. He is a reviewer of multiple IEEE journals and conferences. Dr. Chaloun was the recipient of the Best Paper Award at the German Microwave Conference in 2015. In 2016, he was also the recipient of the Best Paper in the IET Microwaves, Antennas & Propagation.

SUSANNE BRANDL (Graduate Student Member, IEEE) received the M.Sc. degree from Saarland University, Saarbrücken, Germany. She is currently working toward the Ph.D. degree in electrical engineering, Ulm University, Ulm, Germany. In 2019, she joined the Institute of Microwave Engineering. Her research interests include reflectarrays, frequency-selective surfaces, and packaging and interconnect technology for antenna array systems, with focus on the upper millimeter-wave range above 200 GHz.

NORBERT AMBROSIUS studied mechanical engineering with RWTH Aachen University. He received the Dipl.-Ing degree in 2013. He started his career as a Project Manager with Technology Development Department, LPKF Laser & Electronics AG, where he developed the LIDE process. In 2021, he became the Department Manager, Technology Development, LPKF and in that role, he is responsible for the process and technology development of LIDE technology. He is an inventor and co-inventor of multiple patents in that field.

HOLGER MAUNE (Senior Member, IEEE) was born in Cologne, Germany, in 1981. He received the Dipl.-Ing., Dr.-Ing., and venia legend degrees in communications engineering from Technische Universität Darmstadt, Darmstadt, Germany, in 2006, 2011, and 2020, respectively. Since 2021, he has been a Full Professor of electrical engineering and holds the Chair of Microwave and Communication Engineering with the University of Magdeburg, Magdeburg, Germany. His research interests include reconfigurable smart radio frequency (RF) systems based on electronically tunable microwave components, such as phase shifters, adaptive matching networks, tunable filters, duplexer, and multiband antennas. Their integration into system components, such as adaptively matched power amplifiers, reconfigurable RF front ends, or fully integrated electronically beam-steering transceiver antenna arrays, is in the focus of the work.

CHRISTIAN WALDSCHMIDT (Fellow, IEEE) received the Dipl.-Ing. (M.S.E.E.) and Dr.-Ing. (Ph.D.E.E.) degrees from University Karlsruhe (TH), Karlsruhe, Germany, in 2001 and 2004, respectively. From 2001 to 2004, he was a Research Assistant with the Institut für Höchstfrequenztechnik and Elektronik (IHE), Universität Karlsruhe (TH). Since 2004, he has been with Robert Bosch GmbH, in the business units Corporate Research and Chassis Systems. He was heading different research and development teams in microwave engineering, RF-sensing, and automotive radar. In 2013, he returned to academia. He was appointed as the Director of the Institute of Microwave Engineering, University Ulm, Ulm, Germany, as a Full Professor. He authored or coauthored more than 250 scientific publications and more than 20 patents. His research interests include radar and RF-sensing, mm-wave and submillimeter-wave engineering, antennas and antenna arrays, and RF and array signal processing. He is a Member of the executive committee board of the German MTT/AP joint chapter and a Member of the German Information Technology Society. He was the Chair of the IEEE MTT-29 Technical Committee on Microwave Aerospace Systems and the MTT-27 Technical Committee on Wireless Enabled Automotive and Vehicular Applications. He was a two-time TPC chair and general chair of the IEEE MTT International Conference on Microwaves for Intelligent Mobility. Since 2018, he has been an Associate Editor for IEEE MICROWAVE WIRELESS COMPONENTS LETTERS. He is a reviewer of multiple IEEE transactions and many IEEE conferences in the field of microwaves. He is a recipient of 12 best paper awards.

KEVIN KRÖHNERT studied electrical engineering with the Technical University of Berlin, Berlin, Germany. He received the M.Sc. degree in 2014. In 2008, he started to work as a Student Assistant with Fraunhofer IZM, Berlin, Germany. After his graduation in 2014, he continued to work for Fraunhofer IZM. He is responsible for the PVD, dicing and grinding processes, and the acquisition and realization of various projects regarding microtechnology with the focus on glass interposer and wafer level packaging.